Available online at www.sciencedirect.com

ScienceDirect

Journal of Economic Theory 172 (2017) 451–477

JOURNAL OF Economic Theory

www.elsevier.com/locate/jet

Shilnikov chaos in the Lucas model of endogenous growth ☆

Giovanni Bella *, Paolo Mattana, Beatrice Venturi

Department of Economics and Business, University of Cagliari, Via S. Ignazio, 17, 09123 Cagliari, Italy

Received 24 July 2015; final version received 21 June 2017; accepted 30 September 2017
Available online 10 October 2017

Abstract

This paper shows that chaotic dynamics and global indeterminacy may characterize the Lucas (1988) endogenous growth model in its local determinacy region of the parameter space. This is achieved by means of the Shilnikov (1965) theorem, which exploits the existence of a family of homoclinic orbits doubly asymptotic to the balanced growth path, when it is a saddle-focus. The economic implications of these results are also discussed.

JEL classification: C53; C62; O41; E32

Keywords: Lucas model; Shilnikov chaos; Global indeterminacy; History *versus* expectations

1. Introduction

It is now well understood that the equilibrium conditions of the intertemporal general equilibrium theory do not always determine the perfect foresight path uniquely. Such indeterminacy of the equilibrium is commonly investigated by means of the local analysis: if the number of stable roots of the linearization matrix (evaluated at a hyperbolic stationary point, which may correspond to a balanced growth path) exceeds the number of state (predetermined) variables, then

☆ The authors are grateful to an associate editor and three anonymous referees of this journal for their insightful comments that have greatly improved the quality of the paper. The authors also thank Angelo Antoci for his constructive suggestions.

* Corresponding author.
E-mail addresses: bella@unica.it (G. Bella), mattana@unica.it (P. Mattana), venturi@unica.it (B. Venturi).

https://doi.org/10.1016/j.jet.2017.09.010
0022-0531/

there exists a *continuum* of equilibrium paths converging to the stationary point, each of which departing from the initial choice of the jumping variables. In this case, the equilibrium is said to be locally indeterminate.[1] However, excluding multiple equilibrium paths in the local dynamics does not rule out the existence of other perfect foresight paths in the large. A global analysis may uncover the existence of multiple perfect foresight paths that do not stay in a neighborhood of a stationary point; the system may be locally determinate but globally indeterminate.[2] Furthermore, such a global analysis might reveal the possibility of chaotic dynamics. If this happens, two economies initially endowed with the same level of the predetermined variables may follow over time different equilibrium paths, depending on the choice of the jump variables. Despite that the mathematical theory of chaos in continuous time is well-developed, the possibility of chaotic dynamics in economics is, to the best of our knowledge, restricted to discrete-time models.[3]

This paper shows that the system of dynamic laws characterizing the competitive solution of the Lucas (1988) model admits chaotic solutions and gives rise to global indeterminacy in the region of the parameter space where the equilibrium is locally determinate. The mathematical theory behind these results exploits the existence of a family of homoclinic orbits doubly asymptotic to a saddle-focus in $\mathbb{R}^3$. The striking complexity of the dynamics near these homoclinic orbits has been discovered and investigated by Shilnikov (1965), who has shown that, if the associated saddle quantity is positive, infinitely many saddle limit cycles coexist at the bifurcation point; each of these saddle limit cycles has both stable and unstable manifolds, determining high sensitivity to initial conditions and irregular transitional dynamics.[4]

Implications are noteworthy. The Lucas (1988) model has been extraordinarily popular among growth theory researchers during the past decades, playing a role of paramount importance in the attempt to understand the determinants of growth, and the mechanism governing transitional dynamics in perturbed economies. This framework is also still widely considered as a fundamental benchmark for ongoing research (Chilarescu and Viasu, 2016; Lucas and Moll, 2014; Manuelli and Seshadri, 2014) and devising policy (Naz et al., 2016). Hence, the discovery of regions in the parameter space where long-run non-balanced growth emerges as a possible solution of the model is worth knowing. This paper also presents important implications for the field of business cycles (see Farmer, 2016, for a recent survey). As a matter of fact, our results confirm that irregular deterministic oscillating solutions can endogenously emerge as perfect-foresight paths. A further conclusion of our paper is that long-run growth and cycles are generated by the same process.[5] This is an important innovation with regard to a long tradition in macroeconomics, suggesting that the dynamics of real variables may be decomposed into a long-run "secular" and a transitory "cyclical" component.

[1] There is a huge bulk of literature using this approach. An extensive outline is in Benhabib and Farmer (1999).

[2] The idea of *global indeterminacy* dates back, at least, to the seminal works of Krugman (1991) and Matsuyama (1991). In the footsteps of these contributions, there is a fast-growing literature stressing the importance of global analysis in contexts in which equilibrium selection is not unequivocally determined by the initial values of the state variables. Examples are Benhabib and Eusepi (2005), Benhabib et al. (2008), Coury and Wen (2009), Mattana et al. (2009), Bella and Mattana (2014), Antoci et al. (2014).

[3] See Nishimura et al. (1994), Nishimura and Yano (1995), Mitra (2001), Boldrin et al. (2001), Mitra and Nishimura (2001a, 2001b), Khan and Mitra (2005), Gardini et al. (2008).

[4] To the best of our knowledge, the Shilnikov homoclinic bifurcation theorem, largely used in physics, biology, electronic circuits, chemistry and mechanical engineering, has not found application in economics.

[5] This issue is extensively explored in the literature. An original point of view is provided in Matsuyama (1999, 2001) and Wälde (2005). Interestingly in our perspective, the model in Matsuyama (1999) is further explored by Gardini et al. (2008) who fully characterize the possibility of chaotic dynamics.

We can now present the plan of the paper. The second section recalls the three-dimensional system of first-order differential equations characterizing the competitive solution of the Lucas (1988) model, as obtained by Benhabib and Perli (1994). We also review what is known about local stability of this model in the literature. In the third section, we show how parameters can be restricted so that the three-dimensional dynamics characterizing the competitive solution of the model satisfies the requirements of the Shilnikov (1965) theorem. An example of chaotic dynamics is also presented. The fourth section discusses the economic implications of our results. The conclusion reassesses the main findings of the paper.

2. The model

2.1. The dynamic system and the steady state

Benhabib and Perli (1994), BP henceforth, show that the dynamic system

$$\begin{aligned} \dot{x} &= Ax^{\beta}u^{1-\beta} + \tfrac{\delta(1-\beta+\gamma)}{\beta-1}(1-u)x - qx \\ \dot{u} &= \tfrac{\delta(\beta-\gamma)}{\beta}u^2 + \tfrac{\delta(1-\beta+\gamma)}{\beta}u - qu \\ \dot{q} &= q^2 + A\tfrac{\beta-\sigma}{\sigma}x^{\beta-1}u^{1-\beta}q - \tfrac{\rho}{\sigma}q \end{aligned} \tag{$\mathcal{S}$}$$

characterizes the equilibrium paths of the Lucas (1988) model, with $x, q > 0$ and $u \in (0, 1)$. Notation reads as follows: $x = kh^{-\frac{1-\beta+\gamma}{1-\beta}}$ and $q = \frac{c}{k}$ denote stationarizing transformations of the original variables, namely physical capital (k), human capital (h) and consumption (c). Additionally, u is the fraction of total time allocated to goods production. Since total time is normalized to one, $(1-u)$ is the fraction of total time devoted to the sector of education. By definition, x is the predetermined variable, whereas u and q are the jump variables of the system. Parameters are as follows. $(A, \delta) \in \mathbb{R}^2_{++}$ measure the technological levels in the physical capital and human capital sectors, respectively; $\beta \in (0, 1)$ is the share of physical capital in the goods sector; $\rho \in \mathbb{R}_{++}$ is the time preference rate; $\sigma \in \mathbb{R}_+$ is the inverse of the intertemporal elasticity of substitution, with $\sigma \neq 1$. Finally, $\gamma \in \mathbb{R}_{++}$ is the externality parameter in the production of human capital. Therefore, the set of parameters $\theta \equiv (A, \beta, \gamma, \delta, \rho, \sigma)$ lives inside $\Theta = \mathbb{R}_{++} \times (0, 1) \times \mathbb{R}^3_{++} \times \mathbb{R}_+ - \{1\}$.

Let now

$$x^* = \left[\frac{\beta(\rho/\sigma) - \delta(1-\beta+\gamma) - \delta(\beta-\gamma)u^*}{A\beta(\beta-\sigma)/\sigma}\right]^{1/(\beta-1)} u^* \tag{1a}$$

$$u^* = 1 - \frac{(1-\beta)(\rho-\delta)}{\delta\left[\gamma - \sigma(1-\beta+\gamma)\right]} \tag{1b}$$

$$q^* = \frac{\delta(1-\beta+\gamma)}{\beta} + \frac{\delta(\beta-\gamma)}{\beta}u^* \tag{1c}$$

be values of (x, u, q) such that $\dot{x} = \dot{u} = \dot{q} = 0$. BP demonstrate that $P^* \equiv (x^*, u^*, q^*)$ is the only possible interior steady state of system $\mathcal{S}$ when $\rho \neq \delta$ and $\sigma \neq \gamma/(1-\beta+\gamma)$. Furthermore, when the set of parameters θ is located in either one of the following two subsets of Θ

$$\Theta_1 = \left\{\theta \in \Theta : \rho \in (0, \delta); \sigma > 1 - \frac{\rho(1-\beta)}{\delta(1-\beta+\gamma)}\right\} \tag{2}$$

$$\Theta_2 = \left\{\theta \in \Theta : \rho \in (\delta, \delta + \frac{\delta\gamma}{1-\beta}), \sigma \in (0, 1 - \frac{\rho(1-\beta)}{\delta(1-\beta+\gamma)})\right\} \tag{3}$$

P^* is unique, and $0 < u^* < 1$. BP also show that the growth rate of the economy at the unique steady state is

$$g^* = \delta \tfrac{1-\beta+\gamma}{1-\beta}(1-u^*) \tag{4}$$

and that, at the steady state, the TVC is satisfied.

2.2. Stability properties

Let now $\mathbf{J}$ denote the Jacobian matrix of system $\mathcal{S}$, evaluated at P^*. The eigenvalues of $\mathbf{J}$ are the solutions of the characteristic equation

$$\det(\mu\mathbf{I}-\mathbf{J}) = \mu^3 - \mathrm{Tr}(\mathbf{J})\mu^2 + \mathrm{B}(\mathbf{J})\mu - \mathrm{Det}(\mathbf{J}) \tag{5}$$

where $\mathbf{I}$ is the identity matrix. $\mathrm{Tr}(\mathbf{J})$ and $\mathrm{Det}(\mathbf{J})$ are Trace and Determinant of $\mathbf{J}$, respectively. $\mathrm{B}(\mathbf{J})$ is the sum of principal minors of order 2. The explicit values are reported in Appendix A.1.1.

By applying the Routh–Hurwitz criterion, BP obtain the following.

Proposition 1. *Let $\theta \in \Theta_1$. Then the equilibrium path is locally unique*: $\mathbf{J}$ *has one negative eigenvalue and two eigenvalues with positive real parts. Let now $\theta \in \Theta_2$. Then: i) if $\gamma > \beta$, there is always a continuum of equilibria*: $\mathbf{J}$ *has one positive eigenvalue and two eigenvalues with negative real parts; ii) if $0 < \gamma \leq \beta$, there exist two subsets, Θ_2^A and Θ_2^B, such that if $\theta \in \Theta_2^A$, there is again a continuum of equilibria*: $\mathbf{J}$ *has one positive eigenvalue and two eigenvalues with negative real parts, whereas if $\theta \in \Theta_2^B$, there are no equilibria converging to the steady state:* $\mathbf{J}$ *has three eigenvalues with positive real parts.*

Mattana and Venturi (1999) and Nishimura and Shigoka (2006) take Proposition 1 further and prove conditions for system $\mathcal{S}$ to undergo supercritical and subcritical Hopf bifurcations for parameters values at the boundary of the Θ_2^A and Θ_2^B subsets. This possibility, already conjectured by BP, implies that stable and unstable closed orbits can emerge around the steady state. Barnett and Ghosh (2014) provide additional information on the properties of these closed orbits, by numerically locating the regions in the parameter space giving rise to branch-point and limit point of cycles.

Given the strong nonlinearities characterizing system $\mathcal{S}$, very few indications on how solution trajectories behave *in the large* are available in the literature. These results are typically obtained for the case $\theta \in \Theta_2$, under strong restrictions in the parameter space. Bethmann and Reiß (2012), for example, prove global saddle-path stability in the special case of $\sigma = 1$, namely when a stream of *logarithmic* utility is maximized over time.[6]

To the best of our knowledge, no exploration of the global dynamics exists when $\theta \in \Theta_1$. This paper focuses on this local determinacy region of the parameter space, and shows that perfect-foresight chaotic solution trajectories, remained hidden in the local approach, may emerge.

3. Shilnikov chaos in the Lucas model

Chen and Zhou (2011) provide the following version of the original Shilnikov (1965) theorem.

[6] Xie (1994) shows that if $\sigma = \beta$, and if $\gamma > \beta$, there exists a *continuum* of equilibria converging to the balanced growth path in the original $\mathbb{R}^4$ dimension.

Theorem 1. *Consider the dynamic system*

$$\frac{dY}{dt} = f(Y, \alpha), \quad Y \in \mathbb{R}^3, \quad \alpha \in \mathbb{R}^1$$

with f sufficiently smooth. Assume f has a hyperbolic saddle-focus equilibrium point $Y_0 = 0$ at $\alpha = 0$ implying that eigenvalues of the Jacobian $A = Df$ are of the form η and $\tau \pm \omega i$ where η, τ and ω are real constants with $\eta\tau < 0$. Assume that the following conditions also hold:

$(H.1)$ *the saddle quantity $SQ \equiv |\eta| - |\tau| > 0$;*
$(H.2)$ *there exists a homoclinic orbit Γ_0 based at Y_0. Then:*
- (1) *the Shilnikov map,*[7] *defined in the neighborhood of the homoclinic orbit of the system, possesses an infinite number of Smale horseshoes in its discrete dynamics;*
- (2) *for any sufficiently small C^1-perturbation g of f, the perturbed system has at least a finite number of Smale horseshoes in the discrete dynamics of the Shilnikov map, defined in the neighborhood of the homoclinic orbit;*
- (3) *both the original and the perturbed system exhibit horseshoe chaos.*

3.1. A saddle-focus with $SQ > 0$ in the Lucas model

The application of Theorem 1 to system $\mathcal{S}$ requires that several conditions be fulfilled. Specifically, we need that: i) system $\mathcal{S}$ possesses a hyperbolic saddle-focus equilibrium point; *ii*) in the case of the saddle-focus equilibrium, SQ be positive; *iii*) in the case of the saddle-focus equilibrium, with $SQ > 0$, there exists a homoclinic orbit, connecting the saddle-focus to itself. In this subsection, we show that system $\mathcal{S}$ supports the existence of a saddle-focus equilibrium with $SQ > 0$.

For the steady state of system $\mathcal{S}$ to be a saddle-focus, we need to show that $\mathbf{J}$ has a pair of roots with non-zero imaginary part. Solving the characteristic equation (5) by Cardano's formula provides the following solutions

$$\mu_1 = \frac{\mathrm{Tr}(\mathbf{J})}{3} + v + z = \eta$$
$$\mu_{2,3} = \frac{\mathrm{Tr}(\mathbf{J})}{3} - \frac{v+z}{2} \pm \sqrt{3}\frac{v-z}{2} i = \tau \pm \omega i$$

with $v = \sqrt[3]{-\frac{n}{2} + \sqrt{\Delta}}$ and $z = \sqrt[3]{-\frac{n}{2} - \sqrt{\Delta}}$, where

$$\Delta = \left(\frac{m}{3}\right)^3 + \left(\frac{n}{2}\right)^2 \tag{6}$$

is the discriminant. Furthermore, $m = \frac{3\mathrm{B}(\mathbf{J}) - \mathrm{Tr}(\mathbf{J})^2}{3}$ and $n = -\mathrm{Det}(\mathbf{J}) - 2\frac{\mathrm{Tr}(\mathbf{J})^3}{27} + \frac{\mathrm{Tr}(\mathbf{J})\mathrm{B}(\mathbf{J})}{3}$. $i = \sqrt{-1}$ is standard notation for imaginary unit.

Therefore, the following can be proved.

Proposition 2. *Let $\Omega \equiv \left\{\theta \in \Theta_1 : n \in \left(n_2 = \frac{2\sqrt{3}}{9}\sqrt{-m^3}, \infty\right)\right\}$. Then, if $\theta \in \Omega$, P^* is a saddle-focus equilibrium with $SQ > 0$, $\Omega \neq \varnothing$.*

---

[7] In the field of dynamic systems, a first recurrence map, or Poincaré map, is the intersection of a periodic orbit in the state space of a continuous dynamic system with a certain lower-dimensional subspace, called the Poincaré section, transversal to the flow of the system. The 2-dimensional Poincaré map is also called the Shilnikov map.

Proof. In Appendix A.1.2, we show that inside Θ_1, m is always negative. Consequently, Δ is positive when

$$n \in \left(-\infty, n_1 = -\tfrac{2\sqrt{3}}{9}\sqrt{-m^3}\right) \cup \left(n_2 = \tfrac{2\sqrt{3}}{9}\sqrt{-m^3}, \infty\right)$$

Furthermore, from the explicit formula for SQ (cf. Appendix A.1.3), we see that when $n > n_2$, $SQ > 0$ (cf. Appendix A.1.4). The statements in Proposition are therefore implied. The discussion below completes the proof by showing that $\Omega \neq \varnothing$. □

We observe that in the transition to the Ω parametric set, the dynamics of system $\mathcal{S}$ undergoes a topological change. We find therefore useful to approach the rest of this discussion by using the logic of the bifurcation theory. Let therefore $(\beta, \delta, \rho, \sigma)$ be a 4-tuple of exogenously given structural parameters, and assume γ be the bifurcation parameter.[8] Hence,

Corollary 1. *Recall Proposition 2. Let $\gamma = \hat{\gamma}$ be the critical value of the externality factor at which $\Delta = SQ = 0$. Then, if $\gamma > \hat{\gamma}$, P^* is a saddle-focus equilibrium with $SQ > 0$.*

Proof. Given the 4-tuple $(\beta, \delta, \rho, \sigma)$, n and m are two parametric functions only depending on γ. In Appendix A.2.2 and A.2.3, we show that $\frac{dn}{d\gamma} > 0$ and $\frac{dm}{d\gamma} < 0$. Then, if $\gamma > \hat{\gamma}$, $n > n_2$ and $\Delta > 0$. Furthermore, since in the proof of Proposition 2 we have shown that $SQ > 0$ for any $n > n_2$, and since Ω is an open set, the result in Proposition is implied. □

Corollary 1 states that there is a lower threshold for γ below which, given a 4-tuple $(\beta, \delta, \rho, \sigma)$, we cannot have a saddle-focus equilibrium with $SQ > 0$. This result is further investigated in the discussion below, where we achieve more information on the region where Ω is located inside Θ_1. The focal point of our analysis is that, as shown in Appendix A.2.1, the bifurcation $\Delta = SQ = 0$ occurs along the following parametric hypersurface

$$\Phi \equiv \mathrm{B}(\mathbf{J}) + \mathrm{Tr}(\mathbf{J})^2 = 0 \tag{7}$$

Expression (7) has a number of useful properties which will lead us toward a sufficiently informative characterization of the boundaries of Ω inside Θ_1.

From the formulas for $\mathrm{B}(\mathbf{J})$ and $\mathrm{Tr}(\mathbf{J})$ in Appendix A.1.1, it is easy to verify that $\Phi = 0$ implies the following quadratic expression in u^*

$$\left[\beta\left(\beta - \hat{\gamma}\right) + \left(2\beta - \hat{\gamma}\right)^2\right] u^{*2} - \beta\hat{\gamma}u^* - \left(1 - \beta - \hat{\gamma}\right) = 0 \tag{8}$$

where $\hat{\gamma}$ is as in Corollary 1. Solving (8), we obtain two solutions for u^*, one of which is negative, and is therefore discarded. Using (1b), the other solution can be written as

$$\frac{\rho}{\delta} = 1 + \frac{\hat{\gamma} - \sigma\left(1 - \beta + \hat{\gamma}\right)}{1 - \beta} + \frac{1}{2}\frac{\left(\beta - 2\hat{\gamma} + \sqrt{21\beta^2 - 20\beta\hat{\gamma} + 4\hat{\gamma}^2}\right)\left(1 - \beta + \hat{\gamma}\right)\left[\hat{\gamma} - \sigma\left(1 - \beta + \hat{\gamma}\right)\right]}{\beta(1 - \beta)\left(5\beta - 4\hat{\gamma}\right)} \tag{9}$$

which represents all possible parametric combinations giving rise to the $\Delta = SQ = 0$ bifurcation in the 4-dimensional $(\beta, \hat{\gamma}, \frac{\rho}{\delta}, \sigma)$ space.[9] Finally, substituting (9) into (6), we obtain the simple three-dimensional function

[8] Notice that the parameter A simplifies out in all relevant computations.

[9] Notice that there is no need to impose the restriction $(5\beta - 4\gamma) \neq 0$, since the singularity can be removed.

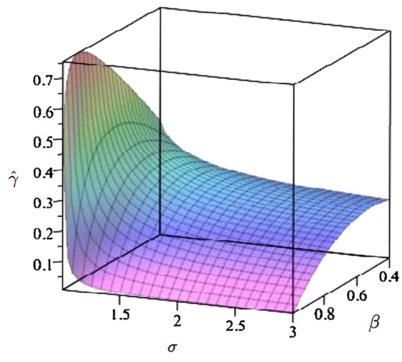

Fig. 1. $(\beta, \hat{\gamma}, \sigma)$ combinations such that $\Delta = SQ = 0$.

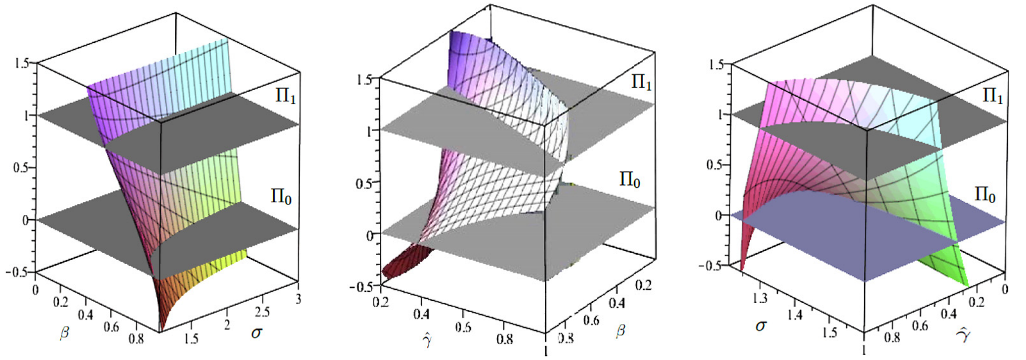

Fig. 2. Values of (ρ/δ) such that $\Delta = SQ = 0$.

$$\sigma = \frac{(5\beta^2 - 4\beta\hat{\gamma} + \hat{\gamma}^2)\beta\hat{\gamma}}{3\beta^4 - 2\beta^3\hat{\gamma} - 3\beta^3 + 7\beta^2\hat{\gamma} - 5\beta\hat{\gamma}^2 + \hat{\gamma}^3} \tag{10}$$

giving rise to Fig. 1 where, for convenience of discussion, $\hat{\gamma}$ is on the vertical axis.[10] Fig. 1 provides interesting details on the values of the parameters at which Δ and SQ simultaneously vanish. In particular, notice that $\hat{\gamma}$ increases sharply when σ approaches unity, and assumes low values only for large β. Since, by Corollary 1, Δ and SQ are both positive for any $\gamma > \hat{\gamma}$, we also have

Remark 1. Ω is located above the surface in Fig. 1.

However, before drawing definitive conclusions, we also need to delimit the regions of the parametric surface in Fig. 1 actually belonging to the Θ_1 set. This can be done by discarding coordinates $(\beta, \hat{\gamma}, \sigma)$ which do not imply $\frac{\rho}{\delta} \in (0, 1)$ in equation (9). By using (9) and (10) we can obtain the three (interconnected) parametric surfaces plotted in Fig. 2 along with the $\frac{\rho}{\delta} = 0$ and $\frac{\rho}{\delta} = 1$ planes (respectively denoted by Π_0 and Π_1).

10 Notice that we restrict our analysis to $\sigma > 1$. As a matter of fact, our simulations reveal that Δ is always negative when $\sigma < 1$. Furthermore, to avoid the representation of numerical anomalies, coordinates are adjusted so that $\beta > 0.4$.

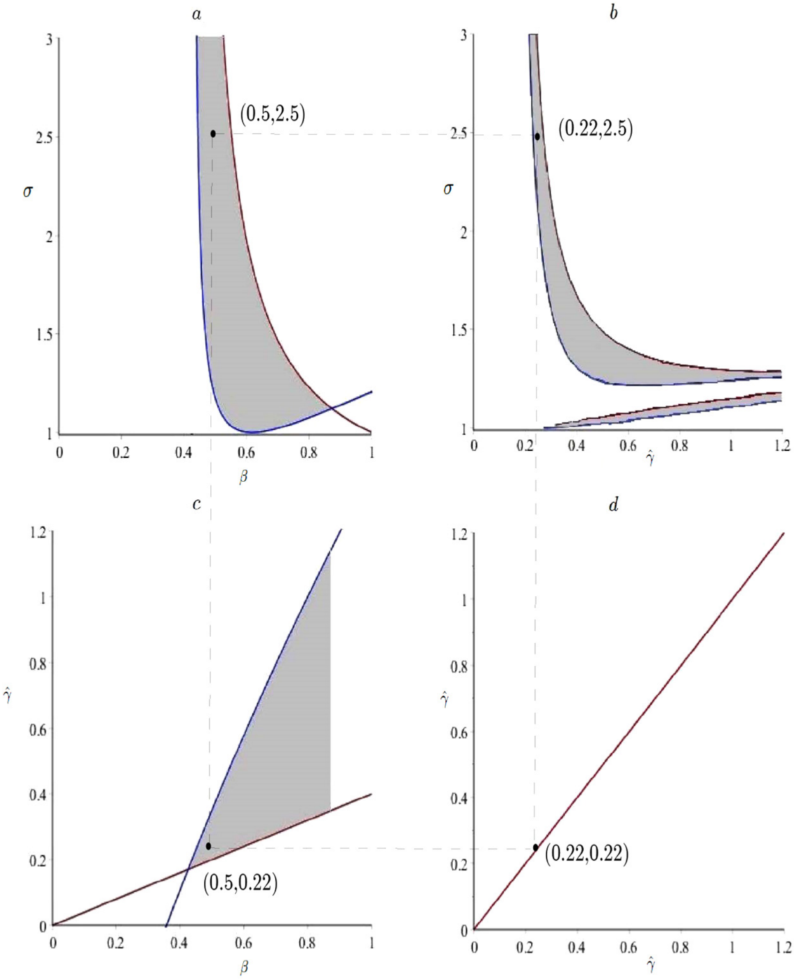

Fig. 3. Set of combinations $(\beta, \hat{\gamma}, \sigma) \subset \Theta_1$. (For interpretation of the colors in this figure, the reader is referred to the web version of this article.)

The intersections of the parametric surfaces in Fig. 2 with Π_0 and Π_1 are finally projected onto the plane (see Fig. 3). The 45-degree line in panel (d) connects the projections. Blue curves denote intersections with the Π_0 plane; red curves intersections with the Π_1 plane.[11] A number of interesting details on the localization of Ω inside Θ_1 follows consequently. In particular, from panels (a) and (c) of Fig. 3, we observe that $\frac{\rho}{\delta} \in (0, 1)$ requires $\beta \in (0.4262, 0.8729)$ and $\hat{\gamma} \in (0.4262, 0.8729)$. The shaded areas in Fig. 3 represent the set of all admissible combinations of $(\beta, \hat{\gamma}, \sigma) \subset \Theta_1$ such that we have a saddle-focus equilibrium with $SQ > 0$. This discussion completes the proof of Proposition 2 by showing that $\Omega \neq \varnothing$.

The following example further clarifies the discussion above.

[11] For graphical convenience, in Fig. 3, we limit the plots to $\sigma = 3$. Notice also that both curves Notice that panel (b) in Fig. 3 implies that, for a given $\hat{\gamma}$, there are two values of σ such that $\frac{\rho}{\delta} \in (0, 1)$.

Example 1. Consider $(\beta, \delta, \rho, \sigma) = (0.5, 0.05, 0.023, 2.5)$. From (9) we also have $\hat{\gamma} \simeq 0.22$. Since $\frac{\rho}{\delta} = 0.46 \in (0, 1)$ and $\sigma > 1$, $(\beta, \delta, \hat{\gamma}, \rho, \sigma) \subset \Theta_1$. Therefore, by Corollary 1, we know that for $\gamma > \hat{\gamma}$, P^* is a saddle-focus equilibrium with $SQ > 0$. Set therefore $(\beta, \gamma, \delta, \rho, \sigma) = (0.5, \frac{1}{3}, 0.05, 0.023, 2.5)$. Then

$$\mu_1 \simeq -0.07112$$

$$\mu_{2,3} \simeq 0.06489 \pm 0.01930i$$

with $SQ = |\eta| - |\tau| \simeq 0.00623 > 0$.

3.2. Existence of a chaotic attractor

Once established that there are regions in the parameter space at which P^* is a saddle-focus equilibrium with $SQ > 0$, we now show that system $\mathcal{S}$ admits homoclinic solutions.[12] To this end, we use the method of the undetermined coefficients (Shang and Han, 2005). As detailed in Appendix A.3, the implementation of the method requires first that system $\mathcal{S}$ is put into the normal form

$$\begin{pmatrix} \dot{w}_1 \\ \dot{w}_2 \\ \dot{w}_3 \end{pmatrix} = \begin{bmatrix} \eta & 0 & 0 \\ 0 & \tau & -\omega \\ 0 & \omega & \tau \end{bmatrix} \begin{pmatrix} w_1 \\ w_2 \\ w_3 \end{pmatrix} + \\ + \begin{pmatrix} F_{1a} w_1 w_2 + F_{1b} w_1 w_3 + F_{1c} w_2 w_3 + F_{1d} w_1^2 + F_{1e} w_2^2 + F_{1f} \; w_3^2 \\ F_{2a} w_1 w_2 + F_{2b} w_1 w_3 + F_{2c} w_2 w_3 + F_{2d} w_1^2 + F_{2e} w_2^2 + F_{2f} \; w_3^2 \\ F_{3a} w_1 w_2 + F_{3b} w_1 w_3 + F_{3c} w_2 w_3 + F_{3d} w_1^2 + F_{3e} w_2^2 + F_{3f} \; w_3^2 \end{pmatrix} \tag{11}$$

where $(w_1, w_2, w_3)^{\mathrm{T}}$ is the vector of transformed coordinates, and the $F_{i,j}$ coefficients, $i = 1, 2, 3$ and $j = a, b \ldots f$, are intricate combinations of the original parameters of the model, also depending on the values of the three constants φ_i $i = 1, 2, 3$ arising in the computation of the eigenbasis.

The following statement can be proved.

Lemma 1. *Denote the set* $\Upsilon \equiv \{\theta \in \Omega : \gamma = \gamma_h \in (\hat{\gamma}, \infty)$ *such that* $\mathcal{S}$ *has a homoclinic orbit*$\}$. *Then* $\Upsilon \neq \varnothing$.

Proof. By Proposition 2 and Corollary 1, we know that if $\theta \in \Omega$, and if $\gamma > \hat{\gamma}$, P^* is a saddle-focus equilibrium with $SQ > 0$. As detailed in Appendix A.3, we show that the application of the method of the undetermined coefficients to system $\mathcal{S}$ requires that the expression

[12] Notice that we are looking for homoclinic solutions connecting a (unique) equilibrium to itself in a $\mathbb{R}^3$ ambient space. This aspect puts this paper in a striking different position when compared to a wide variety of other contributions that derive economic insights from the existence of homoclinic connections. As a matter of fact, homoclinic solutions are typically detected via the Bogadanov–Takens or the Kopell–Howard bifurcation theorems in planar systems (or in "well-located"two-dimensional manifolds in n-dimensional ambient spaces) admitting multiple long-run equilibria (Kuznetsov, 2004; Kopell and Howard, 1975). These theorems allow to unfold the global picture of a given system, in a two parameters space, in a neighborhood of a critical equilibrium with a zero eigenvalue of (algebraic) multiplicity two. Examples range from Benhabib et al. (2001), in the context of interest-rate rules in monetary policy, to Sniekers (2016) in the context of the Beveridge cycle literature. The approach can also been found in recent growth theory research (Mattana et al., 2009; Bella and Mattana, 2014). In the special case where the dynamics is Hamiltonian, homoclinic solutions can be characterized without resorting to the Bogdanov–Takens or the Kopell–Howard bifurcation theorems. Notable examples are Matsuyama (1991) and Mortensen (1999).

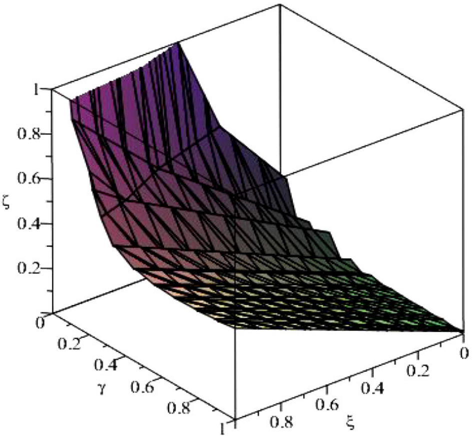

Fig. 4. Combinations of $(\xi, \gamma, \zeta) \in \mathcal{B}_1$ giving rise to a family of homoclinic solutions.

$$\xi = \frac{F_{1c}\psi\zeta + F_{1e}\psi^2 + F_{1f}\zeta^2}{(4\tau - \eta)^2 + \omega^2}(2\tau - \eta) - \frac{F_{1d}}{\eta}\frac{(4\eta^2 + 4\eta\tau + \tau^2 + \omega^2)}{(F_{2d} + F_{3d})(\tau - \omega + 2\eta)}(\psi + \zeta) \tag{12}$$

be satisfied for homoclinic solutions to exist. In (12), (ξ, ψ, ζ) is a triplet of arbitrary constants belonging to $\mathcal{B}_1$, an open set with radius 1 in $\mathbb{R}^3$. Let therefore $(A, \beta, \delta, \rho, \sigma)$ be a 5-tuple of exogenously given structural parameters.[13] Then, the condition for the existence of the homoclinic loop doubly asymptotic to the saddle-focus equilibrium point requires that there exists a $\gamma_h \in \left(\hat{\gamma}, \infty\right)$, with $(A, \beta, \gamma_h, \delta, \rho, \sigma) \in \Omega$, at which (12) is satisfied. The analysis below implies that $\Upsilon \neq \varnothing$. $\square$

We provide now an illustrative example implying the existence of a homoclinic solution of system $\mathcal{S}$.

Example 2. Let $(A, \beta, \delta, \rho, \sigma) \simeq (0.2, 0.5, 0.05, 0.023, 2.5)$ as in Example 1. Recalling (10), this choice implies $\hat{\gamma} = 0.22$. Set $(\varphi_1, \varphi_2, \varphi_3) = \left(\frac{1}{500}, \frac{1}{50}, \frac{1}{20}\right)$. Assume also $\psi = \zeta$. Then equation (12) gives rise to the following surface in the (ξ, γ, ζ) coordinates (see Fig. 4) implying that, given $(\xi, \psi, \zeta) \in \mathcal{B}_1$, there exist values of $\gamma_h > \hat{\gamma} = 0.22$ such that (12) is satisfied. Set finally $\zeta = \frac{1}{5}$ and $\xi \simeq 0.44$. Then, for $\gamma = \gamma_h = 1/3$, system $\mathcal{S}$ has a homoclinic orbit doubly asymptotic to the origin. At $\gamma = \gamma_h$ the economy has $P^* \equiv (x^*, u^*, q^*) \simeq (2.78, 0.85, 0.098)$ and $g^* \simeq 1.31\%$.

Recall now Proposition 2 and Lemma 1. The following holds.

Proposition 3. *Assume $\theta \in \Upsilon$. Then, system $\mathcal{S}$ admits chaotic solution trajectories. If we appropriately choose $(\varphi_1, \varphi_2, \varphi_3)$, the TVC is satisfied.*

Proof. Proposition 2 states that there are regions in the parameter space such that the steady state of system $\mathcal{S}$ is a saddle-focus equilibrium with $SQ > 0$. In addition, Lemma 1 shows that

[13] Notice that, contrarily to the analysis in subsection 3.1, both parameters A and δ are now relevant for the computations.

there exists a critical value of the bifurcation parameter (γ_h) at which a homoclinic orbit, connecting this equilibrium to itself, finally emerges. Therefore, as system $\mathcal{S}$ satisfies all necessary conditions of Theorem 1, chaotic solution trajectories are admitted. In Appendix A.3, we show that the scaling factors φ_i $i = 1, 2, 3$ can be appropriately chosen so that the homoclinic solution satisfies the TVC. □

We provide here below an example of chaotic dynamics arising in the neighborhood of the steady state.

Example 3. Set $(A, \beta, \delta, \rho, \sigma) \simeq (0.2, 0.5, 0.05, 0.02297, 2.5)$, $(\varphi_1, \varphi_2, \varphi_3) = \left(\frac{1}{500}, \frac{1}{50}, \frac{1}{20}\right)$ and $(\xi, \psi, \zeta) \simeq \left(0.44, \frac{1}{5}, \frac{1}{5}\right)$ as in Example 2. Then, if $\gamma_h = 1/3$ there exists a homoclinic orbit doubly asymptotic to the origin. Consider now slightly moving away from the origin. Then, by Shilnikov Theorem, the dynamics exhibits horseshoes chaos. The attractor and its projections are represented in Fig. 5.

Using the mapping defined in Eq. (A.14) in Appendix, we can also go back to the time portraits of the original x, u and q variables of the system. They are depicted in Fig. 6, along with the time portrait of the growth rate of the economy.

Fig. 6 confirms that, after the rupture of the homoclinic orbit, the transitional dynamics of the Lucas (1988) model is globally organized in spiral structures, inducing periods of volatility bursts, irregularly followed by periods of lower-amplitude oscillations.[14] Quite conveniently for a system of dynamic laws governing the economy, the increase in volatility along the spiral attractor is relatively smooth, and never gives rise to explosions.

The existence of a chaotic attractor has additional important implications. The Shilnikov theorem implies that there exists a *continuum* of perfect-foresight equilibrium paths, starting in a wide neighborhood of the steady state. Therefore

Corollary 2. *Let $\theta \in \Upsilon \subset \Omega \subset \Theta_1$. Then, by Proposition 1, the equilibrium is locally determinate. Assume also that conditions in Proposition 3 are satisfied. Then the equilibrium is globally indeterminate.*

Proof. By Shilnikov theorem, given the initial value of the predetermined variable $x(0)$, there exists a *continuum* of initial values of the jump variables $u(0)$ and $q(0)$ belonging to an open neighborhood $\mathcal{U} \subset \mathbb{R}^3$ of P^* such that each path starting on a point in $\mathcal{U}$ continues to stay in the neighborhood of the homoclinic orbit. If conditions in Proposition 3 are satisfied, the TVC holds. Since this *continuum* of equilibria is outside the small neighborhood relevant for the local analysis, the equilibrium is globally indeterminate. □

Corollary 2 complements extant information on the way global indeterminacy occurs in the Lucas (1988) and related models.[15] The property has been proved so far in the literature in

[14] This shape of the time portraits of the variables is peculiar to the Shilnikov spiral attractor. When the phase point gets away from the saddle-focus, we observe rapid and growing oscillations around the equilibrium (cf. also Fig. 6). Instead, once the phase point moves back towards the saddle-focus equilibrium, oscillations start to dampen, and variables exhibit a more quiescent behavior over time.

[15] There is a huge bulk of literature investigating the local indeterminacy properties of the equilibrium for the general case of the two-sector continuous-time endogenous growth model. Significant contributions are Chamley (1993), Benhabib and Farmer (1996), Benhabib and Perli (1994), Benhabib et al. (1994, 2000).

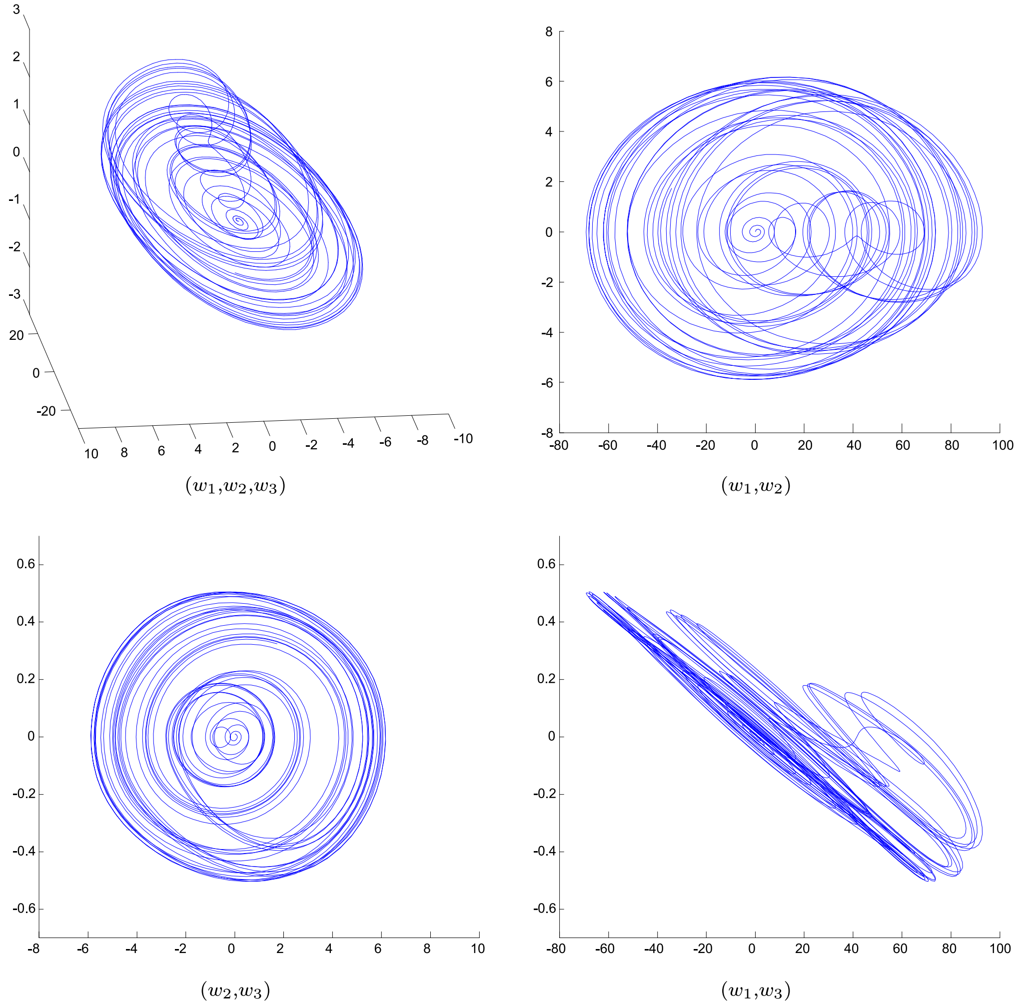

Fig. 5. The attractor and its projections.

connection with: i) the existence of a Hopf cycle around a unique steady state in a well-located bi-dimensional manifold (Mattana and Venturi, 1999; Nishimura and Shigoka, 2006); *ii*) the existence of a homoclinic orbit connecting a saddle point to itself and enclosing a source or a sink (Mino, 2004; Mattana et al., 2009; Bella and Mattana, 2014); *iii*) the existence of different ω-limit sets (Brito and Venditti, 2010; Antoci et al., 2014). In the present analysis, we move a step forward, and show the presence of global indeterminacy for a case in which the dynamics does not converge to a balanced growth configuration or to a cycle. A similar result is reached by Boldrin et al. (2001).

3.3. *Sensitivity analysis*

In this Section, we investigate the sensitivity of the chaotic dynamics to perturbations regarding the bifurcation parameter and the initial conditions. We thus progressively increase/decrease

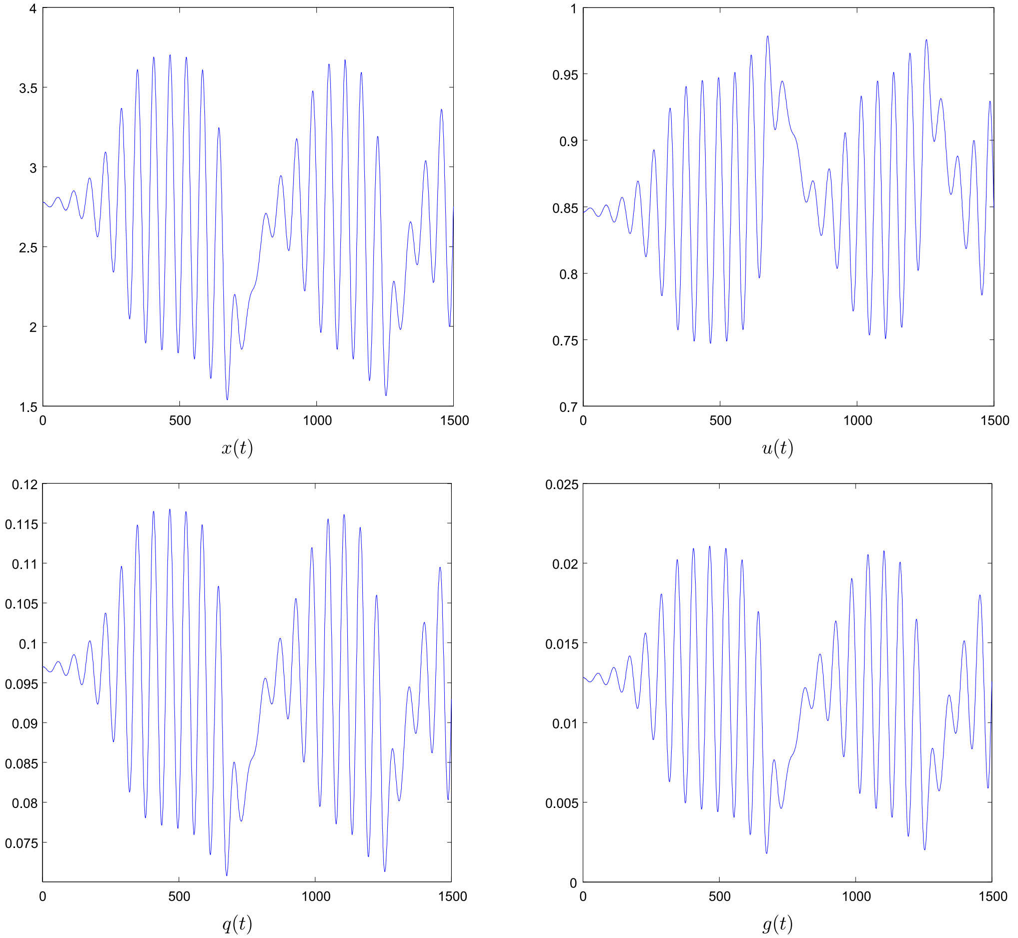

Fig. 6. The time portraits of $x(t)$, $u(t)$, $q(t)$ and $g(t)$.

γ_h by 0.01 (given the initial conditions) and run the iteration, until we find that trajectories escape. As a baseline, we use the parameters in Example 3. This allows to trace the neighborhood of γ_h beyond which the rupture of the attractor occurs. The procedure reveals that, for values of the externality belonging to the interval $(0.32, 0.40)$, solution trajectories do not escape. Notice that this is a quite asymmetric neighborhood of the critical value of the bifurcation parameter $\gamma_h = 1/3$ found in Example 3. It seems that the attractor is quite robust to increases in the bifurcation parameter; conversely, it disappears quickly as soon as the bifurcation parameter decreases.

In Fig. 7, we depict the time portraits of the growth rate of the economy obtained at $\gamma = 0.32$ (red line), and at $\gamma = 0.4$ (green line). We also report the baseline path, corresponding to $\gamma_h = 1/3$ (blue line). It is interesting to observe that the time portraits do not diverge that much at the beginning (in terms of the amplitude of the cycle), when the economy gets away from the steady state, except for the exact location of the cycle-peak; later on differences cumulate over time, and paths start to get apart considerably.

We proceed now to study the effect on the growth rate of the economy due to a change in the initial conditions (given the externality factor). To simplify the discussion, we only consider a

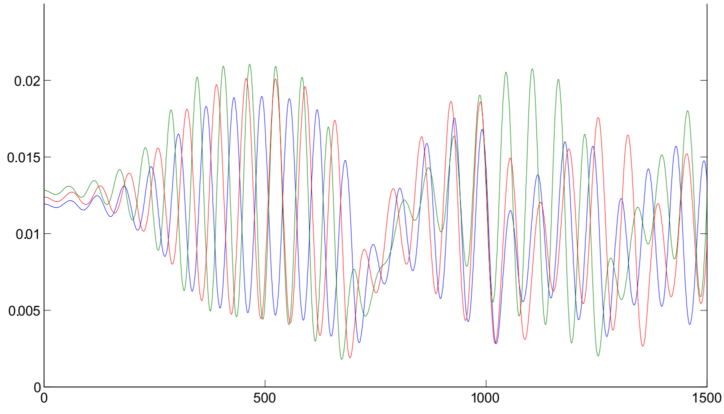

Fig. 7. Effects of a perturbation of γ on the chaotic dynamics of $g(t)$. (For interpretation of the colors in this figure, the reader is referred to the web version of this article.)

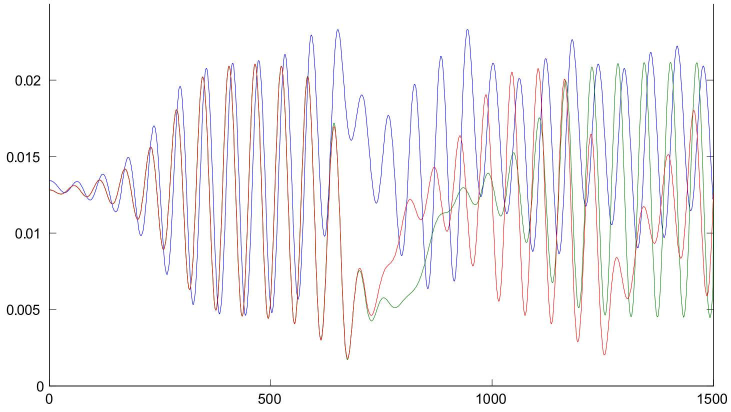

Fig. 8. Effects of a perturbation of $w_1(0)$ on the chaotic dynamics of $g(t)$. (For interpretation of the colors in this figure, the reader is referred to the web version of this article.)

shock in the aggregate capital stock. For this specific parameter set, we observe that the predetermined variable x is strongly related to w_1.[16] As for the case of the externality, we iteratively increase/decrease the initial condition $w_1(0)$ by 0.01, taking fixed the others, and stop as soon as we observe that the dynamics escapes. Running the iterative procedure discussed above with baseline parameters as in Example 3, we find that the rupture of the attractor occurs for values $-5.03 < w_1(0) < 0.140$. This implies that shocks increasing the aggregate capital stock more than 7.19%, or decreasing it for more that 0.81%, the attractor disappears.[17] Fig. 8 depicts the time portrait of the growth rate of the economy obtained for $w_1(0) = -5.03$ (blue curve) and $w_1(0) = 0.140$ (green curve), for given $w_2(0) = w_3(0) = 0.01$. Fig. 8 also reports the original path obtained for the baseline case with $w_1(0) = 0.01$ (red curve).

[16] Specifically, computation of A.14 for baseline parameters in Example 3 gives $\tilde{x} \simeq -0.06273w_1 + 0.002w_2 - 0.00848w_3$.

[17] This asymmetric effect of shocks affecting the state variable of the economy are confirmed in a control example.

Interesting differences appear with regard to the changes in the externality factor γ. Both the cycle amplitude, and the exact location of the cycle peak, are initially not affected by changes in $w_1(0)$, namely when the economy gets away from the steady state along the unstable manifold. Later, as expected, when the solution trajectories point back towards the steady state, the change in the initial condition of w_1 has a dramatic effect on the effective dynamics of the growth rate of the economy.

4. The economics behind chaotic oscillations

It becomes now insightful to develop the economic intuition behind the onset of perfect-foresight chaotic fluctuations. A useful starting point can be gained by reorganizing our findings in terms of a sequence of bifurcations such that one can observe, as parameters are progressively changed, the emergence of a saddle-focus, a homoclinic orbit, and chaos.

In this regard, recall first that we have characterized a critical surface in the parameter space (Fig. 1), such that if parameters are below this surface, the unique steady state of system $\mathcal{S}$ has one negative eigenvalue and two real positive eigenvalues; in this case, in a local perspective, adjustment can only occur along a (generically) steadily converging perfect-foresight path.[18] Conversely, when parameters are above this critical surface, the unique steady state is a saddle-focus and (damped) oscillating converging paths emerge. But what is the economic mechanism behind this phenomenon? Faig (1995) shows that, in the Lucas economy, any decision of a worker to commit the endowment of time is an investment decision that depends on expectations regarding future wages according to the formula

$$w(0) = w(t)e^{-\int_0^t (r(s)-\delta)ds} \quad \text{for all } t \tag{13}$$

where the interest rate $r = A\beta\,(u/x)^{1-\beta}$ is the marginal productivity of physical capital. Therefore the rate at which agents discount the future, $r - \delta$, is the sectoral productivity differential.[19]

Hence, given the externality factor (namely the degree of complementarity across agents' decisions, as in Krugman, 1991, and Matsuyama, 1991), if we are below the surface in Fig. 1, the share of physical capital is relatively low, and returns in the two sectors do not differ that much.[20] An individual adjusting the fraction of time across sectors in response to a shock is motivated to also take distant future into account. This implies that agents are not willing to dispel the benefits of today's education for tomorrow's productivity in the goods sector. As a result, adjustment occurs generically along a steadily converging path. Conversely, if we are above the surface in Fig. 1, for a given level of the degree of complementarity across agents's decisions, the share of physical capital is relatively high, and returns in the two sectors present a wider gap. In this case, an individual does not care about distant future. The benefits of today's education for tomorrow's productivity in the goods sector lose relevance in the perspective of agents' maximization. There is therefore a rapid redeployment of the endowment across sectors, which determines (damped) oscillating paths.

[18] Steady convergence is always warranted when $\gamma = 0$ (Mulligan and Sala-i Martin, 1993; Caballé and Santos, 1993; Faig, 1995). The same result is also obtained when $\gamma \neq 0$ for the centralized solution (Garcia-Castrillo and Sanso, 2000). This implies that, if expectations can be coordinated, the presence of a non competitive element does not prevent the adjustment to be attained in the Lucas economy along a steadily convergent path. See also Boucekkine et al. (2008), Boucekkine and Ruiz-Tamarit (2008), for a global analysis of the optimal growth version of the Lucas (1988) model.

[19] Notice that this crucial element is already pointed out in Krugman (1991).

[20] Recall that in the analysis developed in Subsection 3.1, we have also identified a lower threshold such that, if $(\beta, \hat{\gamma}) < (0.4262, 0.1706)$, the saddle-focus bifurcation cannot occur.

Moreover, in the case parameters are such that P^* is a saddle-focus equilibrium with $SQ > 0$, provided A and δ are also correctly set,[21] there exists a critical value of the degree of complementarity across agents' decisions, $\gamma_h > \hat{\gamma}$, such that a doubly-asymptotic global connection is created between the steady state and itself. In economic terms, this means that the rapid redeployment of the endowment across sectors, implied by the heavy discount of the future, creates a self-sustaining cycle which only terminates after an infinite period of time. In addition, by the Shilnikov (1965) theorem, we have finally shown that in a neighborhood $\mathcal{U} \in \mathbb{R}^3$ of this orbit, there is a *continuum* of aperiodic, and perpetual oscillating, paths around the steady state. The phenomenon is global, and typically implies increasing amplitude oscillations around the steady state at the beginning of the process, when the economy is pushed away from P^* along the unstable manifold; though fluctuations lower their amplitude as we move back towards P^*.

Notice also that a critical ingredient for this bifurcation scenario to occur is that $\sigma > 1$. As clearly pointed out by authors such as Mulligan and Sala-i Martin (1993), Caballé and Santos (1993) and Faig (1995), when preferences are strongly in favor of a smooth consumption path, the adjustment is mainly driven by changes in the allocation of labor across sectors, whereas changes of the saving rate are not considered a convenient option by agents.

We conclude this section by observing that our discussion helps to clarify the role of history and expectations in shaping the way agents generate beliefs about the behavior of other players in the two-sector endogenous growth model.[22] As discussed above, distortions from the optimal path can drive the economy from a state in which history does not matter at all (and the system attains steady convergence towards the unique equilibrium) to a situation where history is so decisive that any small difference at the beginning would magnify over time, so that two economies, even starting contiguously in the initial conditions space, will follow completely different patterns.

5. Conclusions

In this paper we have shown that the standard variant of the Lucas (1988) two-sector endogenous growth model undergoes the homoclinic Shilnikov bifurcation. After the rupture of the homoclinic orbit, the dynamics implied by the model is globally organized in spiral structures, inducing periods of volatility bursts, irregularly followed by periods of lower-amplitude oscillations. Quite conveniently for a system of dynamic laws governing the economy, the increases in volatility along the spiral attractor are relatively smooth, and never give rise to explosions.

We have examined the implications of these results under several perspectives. Firstly, we have discussed a result of global indeterminacy of the equilibrium, implying the existence of a *continuum* of perfect-foresight solution trajectories departing from the same initial condition. Secondly, we have outlined a "route to chaos" describing how, as parameters are tuned, distortions from the optimal path can drive the economy from a state in which history does not matter at all (and the system attains steady convergence towards the unique equilibrium of the system) to a chaotic scenario where history is so decisive that any small difference at the beginning would magnify over time.

[21] Simulations, not reported for the sake of brevity, reveal that there are not combinations of $(\xi, \chi, \psi) \in \mathcal{B}_1$ for $A > 0.53$ and $\delta > 0.26$.

[22] In this regard, we observe that this particular element, firstly pointed out by Krugman (1991) and Matsuyama (1991) in their seminal papers, is still at the forefront of current economic research (Antoci et al., 2014; Acemoglu and Jackson, 2015).

Appendix A

A.1. Proof of Proposition 2 (existence of a saddle-focus)

A.1.1. Recall from BP the Jacobian matrix of system $\mathcal{S}$, evaluated at the steady state $P^* \equiv (x^*, u^*, q^*)$

$$\mathbf{J} = \begin{bmatrix} j_{11}^* & -\frac{x^*}{u^*}\left(j_{11}^* - \delta\frac{1-\beta+\gamma}{1-\beta}u^*\right) & -x^* \\ 0 & \delta\frac{\beta-\gamma}{\beta}u^* & -u^* \\ \frac{\beta-\sigma}{\sigma}\frac{j_{11}^* q^*}{x^*} & -\frac{\beta-\sigma}{\sigma}\frac{j_{11}^* q^*}{u^*} & q^* \end{bmatrix}$$

The single elements of $\mathbf{J}$ are as in BP. Therefore

$$\mathrm{Tr}(\mathbf{J}) = \tfrac{2\beta-\gamma}{\beta}\delta u^*; \quad \mathrm{Det}(\mathbf{J}) = j_{11}^* u^* q^* Q; \quad \mathrm{B}(\mathbf{J}) = j_{11}^* q^* + \tfrac{\beta-\gamma}{\beta}(\delta u^*)^2 \tag{A.1}$$

where $Q = \frac{\delta[\gamma-\sigma(1-\beta+\gamma)]}{\sigma(\beta-1)}$.

A.1.2. Recall that

$$m = \mathrm{B}(\mathbf{J}) - \tfrac{\mathrm{Tr}(\mathbf{J})^2}{3} \tag{A.2}$$

By substituting the expressions for $\mathrm{B}(\mathbf{J})$ and $\mathrm{Tr}(\mathbf{J})$ in (A.1), it is easy to obtain

$$m = j_{11}^* q^* - \frac{(\delta u^*)^2}{3\beta^2}\left[3\beta^2 - 3\gamma\beta + \gamma^2\right]$$

Since $j_{11}^* < 0$, $q^* > 0$ and $3\beta^2 - 3\gamma\beta + \gamma^2 > 0$, it follows that $m < 0$.

A.1.3. Recall from Cardano's formula that

$$\eta = \tfrac{\mathrm{Tr}(\mathbf{J})}{3} + v + z \tag{A.3a}$$

$$\tau = \tfrac{\mathrm{Tr}(\mathbf{J})}{3} - \tfrac{v+z}{2} \tag{A.3b}$$

Therefore, $SQ \equiv |\eta| - |\tau|$ can be rewritten as

$$SQ = \sqrt{\left(\tfrac{\mathrm{Tr}(\mathbf{J})}{3} + v + z\right)^2} - \sqrt{\left(\tfrac{\mathrm{Tr}(\mathbf{J})}{3} - \tfrac{v+z}{2}\right)^2}$$

which is also

$$SQ = \frac{\left(\sqrt{\left(\frac{\mathrm{Tr}(\mathbf{J})}{3}+v+z\right)^2} - \sqrt{\left(\frac{\mathrm{Tr}(\mathbf{J})}{3}-\frac{v+z}{2}\right)^2}\right)\left(\sqrt{\left(\frac{\mathrm{Tr}(\mathbf{J})}{3}+v+z\right)^2} + \sqrt{\left(\frac{\mathrm{Tr}(\mathbf{J})}{3}-\frac{v+z}{2}\right)^2}\right)}{\sqrt{\left(\frac{\mathrm{Tr}(\mathbf{J})}{3}+v+z\right)^2} + \sqrt{\left(\frac{\mathrm{Tr}(\mathbf{J})}{3}-\frac{v+z}{2}\right)^2}} =$$

$$= \frac{\left(\frac{\mathrm{Tr}(\mathbf{J})}{3}+v+z\right)^2 - \left(\frac{\mathrm{Tr}(\mathbf{J})}{3}-\frac{v+z}{2}\right)^2}{\sqrt{\left(\frac{\mathrm{Tr}(\mathbf{J})}{3}+v+z\right)^2} + \sqrt{\left(\frac{\mathrm{Tr}(\mathbf{J})}{3}-\frac{v+z}{2}\right)^2}}$$

Further algebra leads to

$$SQ = \frac{\left(\frac{\mathrm{Tr}(\mathbf{J})}{3}+v+z-\frac{\mathrm{Tr}(\mathbf{J})}{3}+\frac{v+z}{2}\right)\left(\frac{\mathrm{Tr}(\mathbf{J})}{3}+v+z+\frac{\mathrm{Tr}(\mathbf{J})}{3}-\frac{v+z}{2}\right)}{\sqrt{\left(\frac{\mathrm{Tr}(\mathbf{J})}{3}+v+z\right)^2}+\sqrt{\left(\frac{\mathrm{Tr}(\mathbf{J})}{3}-\frac{v+z}{2}\right)^2}} = \frac{\frac{3}{2}(v+z)\left(\frac{2\mathrm{Tr}(\mathbf{J})}{3}+\frac{v+z}{2}\right)}{\sqrt{\left(\frac{\mathrm{Tr}(\mathbf{J})}{3}+v+z\right)^2}+\sqrt{\left(\frac{\mathrm{Tr}(\mathbf{J})}{3}-\frac{v+z}{2}\right)^2}} \tag{A.4}$$

A.1.4. Recall (A.4). By Proposition 1, we know that when $\theta \in \Theta_1$

$$\eta = \frac{\mathrm{Tr}(\mathbf{J})}{3} + v + z < 0$$
$$\tau = \frac{\mathrm{Tr}(\mathbf{J})}{3} - \frac{v+z}{2} > 0$$

Therefore it must be

$$v + z < 0 \tag{A.5}$$

Suppose in fact that $v + z > 0$. Then $\eta < 0$ would imply $\mathrm{Tr}(\mathbf{J}) < 0$. But this would also determine $\tau < 0$. This contradicts Proposition 1. Hence, $SQ > 0$ needs

$$\frac{2}{3}\mathrm{Tr}(\mathbf{J}) + \frac{v+z}{2} < 0 \tag{A.6}$$

We show now that (A.6) is satisfied when $n > 0$. Recall $v = \sqrt[3]{-\frac{n}{2} + \sqrt{\Delta}}$ and $z = \sqrt[3]{-\frac{n}{2} - \sqrt{\Delta}}$. By standard algebra, we obtain

$$v^3 + z^3 = (v+z)\left(v^2 + vz + z^2\right) = -n$$

and since we have just established that, when $\theta \in \Theta_1$, $(v+z) < 0$, we conclude that, for any $n > 0$, $SQ > 0$.

A.2. Properties of the Φ locus in the parameter space

A.2.1. Assume $n = n_2$. From (6) in the main text, recalling (A.4) and (A.5), we obtain the following system

$$\left(\frac{m}{3}\right)^3 + \left(\frac{n_2}{2}\right)^2 = 0 \tag{A.7a}$$
$$\frac{2}{3}\mathrm{Tr}(\mathbf{J}) + \frac{v+z}{2} = 0 \tag{A.7b}$$

Recall the formulas for v and z. When $\Delta = 0$, they reduce to

$$v = z = \sqrt[3]{-\frac{n_2}{2}}$$

Therefore, the expression in (A.7b) can be re-written as

$$\frac{2}{3}\mathrm{Tr}(\mathbf{J}) = \sqrt[3]{\frac{n_2}{2}}$$

that is also

$$\frac{4}{9}\mathrm{Tr}(\mathbf{J})^2 = \sqrt[3]{\left(\frac{n_2}{2}\right)^2}$$

which, by using (A.7a), becomes

$$\frac{4}{9}\mathrm{Tr}(\mathbf{J})^2 = \sqrt[3]{-\left(\frac{m}{3}\right)^3} = -\frac{m}{3}$$

Recalling (A.2), we finally obtain

$$\Phi = \mathrm{B}(\mathbf{J}) + \mathrm{Tr}(\mathbf{J})^2 = 0$$

A.2.2. Recall that

$$n = -\mathrm{Det}(\mathbf{J}) - 2\frac{\mathrm{Tr}(\mathbf{J})^3}{27} + \frac{\mathrm{Tr}(\mathbf{J})\mathrm{B}(\mathbf{J})}{3}$$

Therefore

$$\frac{dn}{d\gamma} = -\frac{d\mathrm{Det}(\mathbf{J})}{d\gamma} - \frac{2\mathrm{Tr}(\mathbf{J})^2}{9}\frac{d\mathrm{Tr}(\mathbf{J})}{d\gamma} + \frac{1}{3}\left(\frac{d\mathrm{Tr}(\mathbf{J})}{d\gamma}\mathrm{B}(\mathbf{J}) + \frac{d\mathrm{B}(\mathbf{J})}{d\gamma}\mathrm{Tr}(\mathbf{J})\right) \tag{A.8}$$

Since $\frac{dj_{11}^*}{d\gamma} = \frac{(1-\beta)^2(\rho-\delta)\sigma}{\beta[\gamma-\sigma(1-\beta+\gamma)]^2} < 0$, $\frac{dq^*}{d\gamma} = \frac{\delta(1-u^*)}{\beta} > 0$, $\frac{dQ}{d\gamma} = -\frac{\delta(1-\sigma)}{\sigma(1-\beta)} > 0$, and $\frac{du^*}{d\gamma} = \frac{(1-\beta)(\rho-\delta)(1-\sigma)}{\delta[\gamma-\sigma(1-\beta+\gamma)]^2} > 0$, we first have

$$\frac{d\mathrm{Det}(\mathbf{J})}{d\gamma} = \frac{dj_{11}^*}{d\gamma}u^*q^*Q + \frac{du^*}{d\gamma}j_{11}^*q^*Q + \frac{dq^*}{d\gamma}j_{11}^*u^*Q + \frac{dQ}{d\gamma}j_{11}^*u^*q^* < 0$$

Furthermore

$$\frac{d\mathrm{Tr}(\mathbf{J})}{d\gamma} = \frac{\delta}{\beta}\left(\frac{2\beta-\gamma}{u^*}\frac{du^*}{d\gamma}u^* - u^*\right) \tag{A.9}$$

implying $\frac{d\mathrm{Tr}(\mathbf{J})}{d\gamma} < 0$ for $\gamma > 2\beta$. We show that $\frac{d\mathrm{Tr}(\mathbf{J})}{d\gamma} < 0$ also for $\gamma < 2\beta$. Let substitute $\frac{du^*}{d\gamma}$ and u^* into (A.9). We obtain

$$\frac{d\mathrm{Tr}(\mathbf{J})}{d\gamma} = \frac{\delta}{\beta}\left[(2\beta-\gamma)\frac{(1-\beta)(\rho-\delta)(1-\sigma)}{\delta[\gamma-\sigma(1-\beta+\gamma)]^2} + \frac{(1-\beta)(\rho-\delta)}{\delta[\gamma-\sigma(1-\beta+\gamma)]} - 1\right]$$

Algebraic calculations lead to the following formula

$$\frac{d\mathrm{Tr}(\mathbf{J})}{d\gamma} = \frac{\delta}{\beta}\left[-\frac{(1-\beta)(\rho-\delta)}{\delta}\frac{\sigma-\beta+\beta(\sigma-1)}{[\gamma-\sigma(1-\beta+\gamma)]^2} - 1\right] < 0 \quad \text{for } \sigma > 1$$

We finally show that also the last element of (A.8), namely

$$\left(\frac{d\mathrm{Tr}(\mathbf{J})}{d\gamma}\mathrm{B}(\mathbf{J}) + \frac{d\mathrm{B}(\mathbf{J})}{d\gamma}\mathrm{Tr}(\mathbf{J})\right) = \frac{d\mathrm{Tr}(\mathbf{J})}{d\gamma}\left(\mathrm{B}(\mathbf{J}) + \frac{d\mathrm{B}(\mathbf{J})}{d\mathrm{Tr}(\mathbf{J})}\mathrm{Tr}(\mathbf{J})\right) \tag{A.10}$$

is positive when $\theta \in \Theta_1$. First of all, using the formula for m, we can see how $\frac{d\mathrm{Tr}(\mathbf{J})}{d\gamma}$ and $\frac{d\mathrm{B}(\mathbf{J})}{d\gamma}$ move together. As a matter of fact, implicit derivative of (A.2) provides

$$\frac{d\mathrm{B}(\mathbf{J})}{d\mathrm{Tr}(\mathbf{J})} = -\frac{\frac{\partial m}{\partial \mathrm{Tr}(\mathbf{J})}}{\frac{\partial m}{\partial \mathrm{B}(\mathbf{J})}} = \frac{2}{3}\mathrm{Tr}(\mathbf{J}) \tag{A.11}$$

Furthermore, substituting (A.11) into (A.10), after algebraic manipulation, we obtain

$$\begin{aligned}\frac{d\mathrm{Tr}(\mathbf{J})}{d\gamma}\left[\mathrm{B}(\mathbf{J}) + \frac{2}{3}\mathrm{Tr}^2(\mathbf{J})\right] &= \frac{d\mathrm{Tr}(\mathbf{J})}{d\gamma}\left[\mathbf{B}(\mathbf{J}) + \frac{2}{3}\mathbf{Tr}(\mathbf{J})^2 + \frac{\mathbf{Tr}(\mathbf{J})^2}{3} - \frac{\mathbf{Tr}(\mathbf{J})^2}{3})\right] = \\ &= \frac{d\mathrm{Tr}(\mathbf{J})}{d\gamma}\left[\mathrm{B}(\mathbf{J}) + \mathrm{Tr}^2(\mathbf{J}) - \frac{1}{3}\mathrm{Tr}^2(\mathbf{J})\right] > 0\end{aligned}$$

Since $\frac{d\mathrm{Tr}(\mathbf{J})}{d\gamma} < 0$, and since in Section A.2.1 we have just shown that $\mathrm{B}(\mathbf{J}) + \mathrm{Tr}^2(\mathbf{J}) = 0$, then $\frac{dn}{d\gamma} > 0$.

A.2.3. From equation (6) in the main text, we can derive

$$\frac{dm}{d\gamma} = -\frac{\frac{\partial \Delta}{\partial \gamma}}{\frac{\partial \Delta}{\partial m}} = -\frac{dm}{d\gamma} - n\frac{\frac{dn}{d\gamma}}{\left(\frac{m}{3}\right)^2}$$

from which it is easy to obtain

$$\frac{dm}{d\gamma} = -\frac{n}{2}\frac{\frac{dn}{d\gamma}}{\left(\frac{m}{3}\right)^2} < 0$$

since in Section A.2.2 we have shown that $\frac{dn}{d\gamma} > 0$.

A.3. Proof of Lemma 1 (existence of a homoclinic orbit)

To show the existence of a family of homoclinic orbits doubly asymptotic to P^*, we use the method of the undetermined coefficients (Shang and Han, 2005). The implementation of the method requires that system $\mathcal{S}$ is put into normal form.

Consider first the variables transformation $\tilde{x} \equiv x - x^*$, $\tilde{u} \equiv u - u^*$, $\tilde{q} = q - q^*$. Taylor expanding, system $\mathcal{S}$ becomes

$$\begin{pmatrix} \dot{\tilde{x}} \\ \dot{\tilde{u}} \\ \dot{\tilde{q}} \end{pmatrix} = \mathbf{J}\begin{pmatrix} \tilde{x} \\ \tilde{u} \\ \tilde{q} \end{pmatrix} + \begin{pmatrix} \tilde{f}_1(\tilde{x}, \tilde{u}, \tilde{q}) \\ \tilde{f}_2(\tilde{x}, \tilde{u}, \tilde{q}) \\ \tilde{f}_3(\tilde{x}, \tilde{u}, \tilde{q}) \end{pmatrix} \tag{A.12}$$

where the various $\tilde{f}_i$ are second-order non linear functions of the variables $(\tilde{x}, \tilde{u}, \tilde{q})$. By Proposition 2, we know that, if $\theta \in \Omega$, $\mathbf{J}$ has one negative real eigenvalue and two complex conjugate eigenvalues with positive real part. Therefore, to obtain the eigenbasis of $\mathbf{J}$ we need to solve the following system

$$\mathbf{Ju} = \tau\mathbf{u} - \omega\mathbf{v}$$
$$\mathbf{Jv} = \omega\mathbf{u} + \tau\mathbf{v}$$
$$\mathbf{Jz} = \eta\mathbf{z}$$

where $\mathbf{u}=[u_1, u_2, u_3]^{\mathrm{T}}$, $\mathbf{v}=[v_1, v_2, v_3]^{\mathrm{T}}$ and $\mathbf{z}=[z_1, z_2, z_3]^{\mathrm{T}}$ are (3×1) vectors. Possible candidates for the eigenvectors are

$$\mathbf{u} = \begin{pmatrix} \frac{(j_{11}^* - \tau + v_3 j_{13}^*)}{\omega}\varphi_1 \\ \frac{v_3 j_{23}^*}{\omega}\varphi_1 \\ \frac{j_{31}^* + (j_{33}^* - \tau)v_3}{\omega}\varphi_1 \end{pmatrix}; \ \mathbf{v} = \begin{pmatrix} \varphi_2 \\ 0 \\ v_3\varphi_2 \end{pmatrix}; \ \mathbf{z} = \begin{pmatrix} \left[j_{23}^* j_{12}^* - (j_{22}^* - \eta) j_{13}^*\right]\varphi_3 \\ -(j_{11}^* - \eta) j_{23}^* \varphi_3 \\ (j_{11}^* - \eta)(j_{22}^* - \eta)\varphi_3 \end{pmatrix} \tag{A.13}$$

where $v_3 = \left[(\eta - j_{11}^*)/j_{13}^*\right]$, and the three free constants φ_i, $i = 1, 2, 3$ can be conveniently chosen. Therefore, using $\mathbf{T} = [\mathbf{z}, \mathbf{u}, \mathbf{v}]$

$$\begin{pmatrix} \tilde{x} \\ \tilde{u} \\ \tilde{q} \end{pmatrix} = \mathbf{T}\begin{pmatrix} w_1 \\ w_2 \\ w_3 \end{pmatrix} \tag{A.14}$$

to operate the coordinate change, we obtain the (truncated) system

$$\begin{pmatrix} \dot{w}_1 \\ \dot{w}_2 \\ \dot{w}_3 \end{pmatrix} = \begin{bmatrix} \eta & 0 & 0 \\ 0 & \tau & -\omega \\ 0 & \omega & \tau \end{bmatrix} \begin{pmatrix} w_1 \\ w_2 \\ w_3 \end{pmatrix} + \tag{A.15}$$
$$+ \begin{pmatrix} F_{1a} w_1 w_2 + F_{1b} w_1 w_3 + F_{1c} w_2 w_3 + F_{1d} w_1^2 + F_{1e} w_2^2 + F_{1f}\ w_3^2 \\ F_{2a} w_1 w_2 + F_{2b} w_1 w_3 + F_{2c} w_2 w_3 + F_{2d} w_1^2 + F_{2e} w_2^2 + F_{2f}\ w_3^2 \\ F_{3a} w_1 w_2 + F_{3b} w_1 w_3 + F_{3c} w_2 w_3 + F_{3d} w_1^2 + F_{3e} w_2^2 + F_{3f}\ w_3^2 \end{pmatrix}$$

where the $F_{i,j}$ coefficients, $i = 1, 2, 3$ and $j = a, b \ldots f$, are intricate combinations of the original parameters of the model, also depending on the values of the three constants φ_i $i = 1, 2, 3$. All coefficients have been computed, but not reported for the sake of a simple representation. They remain available upon request.

To verify whether the system in (A.15) admits a homoclinic bifurcation, we need to provide an explicit polynomial approximation of the analytical expressions of both the one-dimensional stable manifold associated with $\mu_1 = \eta$, and the two-dimensional unstable manifold associated with the complex conjugate eigenvalues $\mu_{2,3} = \tau \pm \omega i$. The method proceeds as follows. Let

$$w_1 = a_0 + \sum_{s=1}^{\infty} a_s e^{s\mu t}; \quad w_2 = b_0 + \sum_{s=1}^{\infty} b_s e^{s\mu t}; \quad w_3 = c_0 + \sum_{s=1}^{\infty} c_s e^{s\mu t} \tag{A.16}$$

represent the analytic expression of the manifold associated with the generic eigenvalue μ, where a_s, b_s, c_s are unknown coefficients. Time derivatives of (A.16) yield

$$\dot{w}_1 = \sum_{s=1}^{\infty} a_s s\mu e^{s\mu t}; \quad \dot{w}_2 = \sum_{s=1}^{\infty} b_s s\mu e^{s\mu t}; \quad \dot{w}_3 = \sum_{s=1}^{\infty} c_s s\mu e^{s\mu t} \tag{A.17}$$

Equating (A.17) with (A.15), and taking into account (A.16), we derive the following expression

$$\begin{aligned} &\begin{matrix} \sum_{s=1}^{\infty} a_s s\mu e^{s\mu t} \\ \sum_{s=1}^{\infty} b_s s\mu e^{s\mu t} \\ \sum_{s=1}^{\infty} c_s s\mu e^{s\mu t} \end{matrix} = \mathbf{J}_N \begin{pmatrix} a_0 + \sum_{s=1}^{\infty} a_s e^{s\mu t} \\ b_0 + \sum_{s=1}^{\infty} b_s e^{s\mu t} \\ c_0 + \sum_{s=1}^{\infty} c_s e^{s\mu t} \end{pmatrix} + \\
&\quad F_{1a}\left(a_0 + \textstyle\sum_{s=1}^{\infty} a_s e^{s\mu t}\right)\left(b_0 + \sum_{s=1}^{\infty} b_s e^{s\mu t}\right) \\
&+ F_{2a}\left(a_0 + \textstyle\sum_{s=1}^{\infty} a_s e^{s\mu t}\right)\left(b_0 + \sum_{s=1}^{\infty} b_s e^{s\mu t}\right) + \\
&\quad F_{3a}\left(a_0 + \textstyle\sum_{s=1}^{\infty} a_s e^{s\mu t}\right)\left(b_0 + \sum_{s=1}^{\infty} b_s e^{s\mu t}\right) \\
&\quad F_{1b}\left(a_0 + \textstyle\sum_{s=1}^{\infty} a_s e^{s\mu t}\right)\left(c_0 + \sum_{s=1}^{\infty} c_s e^{s\mu t}\right) \\
&+ F_{2b}\left(a_0 + \textstyle\sum_{s=1}^{\infty} a_s e^{s\mu t}\right)\left(c_0 + \sum_{s=1}^{\infty} c_s e^{s\mu t}\right) + \\
&\quad F_{3b}\left(a_0 + \textstyle\sum_{s=1}^{\infty} a_s e^{s\mu t}\right)\left(c_0 + \sum_{s=1}^{\infty} c_s e^{s\mu t}\right) \\
&\quad F_{1c}\left(b_0 + \textstyle\sum_{s=1}^{\infty} b_s e^{s\mu t}\right)\left(c_0 + \sum_{s=1}^{\infty} c_s e^{s\mu t}\right) \\
&+ F_{2c}\left(b_0 + \textstyle\sum_{s=1}^{\infty} b_s e^{s\mu t}\right)\left(c_0 + \sum_{s=1}^{\infty} c_s e^{s\mu t}\right) + \\
&\quad F_{3c}\left(b_0 + \textstyle\sum_{s=1}^{\infty} b_s e^{s\mu t}\right)\left(c_0 + \sum_{s=1}^{\infty} c_s e^{s\mu t}\right) \\
&\quad F_{1d}\left(a_0 + \textstyle\sum_{s=1}^{\infty} a_s e^{s\mu t}\right)^2 + F_{1e}\left(b_0 + \sum_{s=1}^{\infty} b_s e^{s\mu t}\right)^2 + F_{1f}\left(c_0 + \sum_{s=1}^{\infty} c_s e^{s\mu t}\right)^2 \\
&+ F_{2d}\left(a_0 + \textstyle\sum_{s=1}^{\infty} a_s e^{s\mu t}\right)^2 + F_{2e}\left(b_0 + \sum_{s=1}^{\infty} b_s e^{s\mu t}\right)^2 + F_{2f}\left(c_0 + \sum_{s=1}^{\infty} c_s e^{s\mu t}\right)^2 \\
&\quad F_{3d}\left(a_0 + \textstyle\sum_{s=1}^{\infty} a_s e^{s\mu t}\right)^2 + F_{3e}\left(b_0 + \sum_{s=1}^{\infty} b_s e^{s\mu t}\right)^2 + F_{3f}\left(c_0 + \sum_{s=1}^{\infty} c_s e^{s\mu t}\right)^2
\end{aligned} \tag{A.18}$$

where $\mathbf{J}_N$ is the linearization matrix in normal form. The system is initialized at the origin. Namely

$$\begin{pmatrix} a_0 \\ b_0 \\ c_0 \end{pmatrix} = \begin{pmatrix} 0 \\ 0 \\ 0 \end{pmatrix} \tag{A.19}$$

The method allows us to derive the unknown coefficients a_s, b_s, c_s of the analytical expression for the homoclinic orbit by comparing elements with the same exponential at the right and left hand sides of (A.18), for s sequentially set to $1, 2...p$ where p is the required degree of approximation. Once the analytical expression is obtained, doubly convergence to $\mathbf{0}$ in $\mathbb{R}^3$, that is to say for $t \to \pm\infty$, has to be searched by tuning the bifurcation parameter γ.

Let us first find the analytical expression for $t > 0$. In this case, the solution trajectory converges to the origin along the stable one-dimensional manifold spanned by the real eigenvalue. The method requires the following steps.

a) Set $s = 1$. From the expression (A.18), the vector $(a_1, b_1, c_1)^T$ can be retrieved by comparing elements with the same exponential $e^{\mu t}$. We have

$$\begin{pmatrix} a_1 \\ b_1 \\ c_1 \end{pmatrix} \mu e^{\mu t} = \mathbf{J}_N \begin{pmatrix} a_0 + a_1 e^{\mu t} \\ b_0 + b_1 e^{\mu t} \\ c_0 + c_1 e^{\mu t} \end{pmatrix}$$

Taking into account (A.19), we also have

$$[\mu \mathbf{I} - \mathbf{J}_N] \begin{pmatrix} a_1 \\ b_1 \\ c_1 \end{pmatrix} = \begin{pmatrix} 0 \\ 0 \\ 0 \end{pmatrix} \tag{A.20}$$

where $\mathbf{I}$ is the identity matrix. Evaluating (A.20) at $\mu = \eta$, and solving for the unknown constants (a_1, b_1, c_1), we obtain the following result

$$\begin{pmatrix} a_1 \\ b_1 \\ c_1 \end{pmatrix} = \begin{pmatrix} \xi \\ 0 \\ 0 \end{pmatrix}$$

where ξ is an arbitrary constant.

b) Set $s = 2$. From (A.18), keeping only elements with $e^{2\mu t}$, we obtain

$$[2\mu \mathbf{I} - \mathbf{J}_N] \begin{pmatrix} a_2 \\ b_2 \\ c_2 \end{pmatrix} = \begin{pmatrix} F_{1d}\xi^2 \\ F_{2d}\xi^2 \\ F_{3d}\xi^2 \end{pmatrix} \tag{A.21}$$

Again, evaluating (A.21) at $\mu = \eta$, and solving for the unknown coefficients a_2, b_2 and c_2, we have

$$\begin{pmatrix} a_2 \\ b_2 \\ c_2 \end{pmatrix} = \xi^2 \begin{bmatrix} \frac{1}{\eta} & 0 & 0 \\ 0 & \frac{\tau+2\eta}{4\eta^2+4\eta\tau+\tau^2+\omega^2} & \frac{\omega}{4\eta^2+4\eta\tau+\tau^2+\omega^2} \\ 0 & -\frac{\omega}{4\eta^2+4\eta\tau+\tau^2+\omega^2} & \frac{\tau+2\eta}{4\eta^2+4\eta\tau+\tau^2+\omega^2} \end{bmatrix} \begin{pmatrix} F_{1d} \\ F_{2d} \\ F_{3d} \end{pmatrix}$$

In general terms, the procedure can be further iterated for $s = 3, 4...p$, till the desired degree of approximated as follows

$$w_1 = \xi e^{-\eta t} + a_2(\xi) e^{-2\eta t}; \; w_2 = b_2(\xi) e^{-2\eta t}; \; w_3 = c_2(\xi) e^{-2\eta t} \tag{A.22}$$

where all parameters are known, and ξ can be arbitrarily fixed.

We can now proceed to obtain the analytical expression of the orbits for $t < 0$. In this case, the solution trajectory converges to the origin along the unstable manifolds spanned by the complex conjugate eigenvalues $\mu_{2,3} = \tau \pm \omega i$. Choosing $\mu_2 = \tau + \omega i$, we obtain the following.

c) Set $s = 1$. From the expression (A.18), the vector $\left(\bar{a}_1, \bar{b}_1, \bar{c}_1\right)^T$ can be retrieved comparing elements with same exponential $e^{\mu t}$. We have

$$\begin{pmatrix} \bar{a}_1 \\ \bar{b}_1 \\ \bar{c}_1 \end{pmatrix} \mu e^{\mu t} = \mathbf{J}_N \begin{pmatrix} \bar{a}_0 + \bar{a}_1 e^{\mu t} \\ \bar{b}_0 + \bar{b}_1 e^{\mu t} \\ \bar{c}_0 + \bar{c}_1 e^{\mu t} \end{pmatrix}$$

Taking into account (A.19), we also have

$$(\mu \mathbf{I} - \mathbf{J}_N) \begin{pmatrix} \bar{a}_1 \\ \bar{b}_1 \\ \bar{c}_1 \end{pmatrix} = \begin{pmatrix} 0 \\ 0 \\ 0 \end{pmatrix} \tag{A.23}$$

Evaluating (A.23) at $\mu_2 = \tau + \omega i$, the values of the unknown coefficients can be obtained as

$$\begin{pmatrix} \bar{a}_1 \\ \bar{b}_1 \\ \bar{c}_1 \end{pmatrix} = \begin{pmatrix} 0 \\ \zeta + \psi i \\ \psi + \zeta i \end{pmatrix}$$

where ζ and ψ are arbitrary constants, and $i = \sqrt{-1}$.

d) Set $s = 2$. From (A.18), matching elements with $e^{2\mu t}$, and simplifying, we can easily derive

$$\begin{pmatrix} \bar{a}_2 2\mu \\ \bar{b}_2 2\mu \\ \bar{c}_2 2\mu \end{pmatrix} = \mathbf{J}_N \begin{pmatrix} \bar{a}_2 \\ \bar{b}_2 \\ \bar{c}_2 \end{pmatrix} + \begin{pmatrix} F_{1c}\bar{b}_1\bar{c}_1 + F_{1e}\bar{b}_1^2 + F_{1f}\bar{c}_1^2 \\ F_{2c}\bar{b}_1\bar{c}_1 + F_{2e}\bar{b}_1^2 + F_{2f}\bar{c}_1^2 \\ F_{3c}\bar{b}_1\bar{c}_1 + F_{3e}\bar{b}_1^2 + F_{3f}\bar{c}_1^2 \end{pmatrix}$$

or

$$[2\lambda \mathbf{I} - \mathbf{J}_N] \begin{pmatrix} \bar{a}_2 \\ \bar{b}_2 \\ \bar{c}_2 \end{pmatrix} = \begin{pmatrix} F_{1c}\bar{b}_1\bar{c}_1 + F_{1e}\bar{b}_1^2 + F_{1f}\bar{c}_1^2 \\ F_{2c}\bar{b}_1\bar{c}_1 + F_{2e}\bar{b}_1^2 + F_{2f}\bar{c}_1^2 \\ F_{3c}\bar{b}_1\bar{c}_1 + F_{3e}\bar{b}_1^2 + F_{3f}\bar{c}_1^2 \end{pmatrix}$$

Evaluating μ at $\mu_2 = \tau + \omega i$, the unknown coefficients $\bar{a}_2$ $\bar{b}_2$ and $\bar{c}_2$ can be obtained as

$$\begin{pmatrix} \bar{a}_2 \\ \bar{b}_2 \\ \bar{c}_2 \end{pmatrix} = [2\mu \mathbf{I} - \mathbf{J}_N]^{-1} \begin{pmatrix} F_{1c}\bar{b}_1\bar{c}_1 + F_{1e}\bar{b}_1^2 + F_{1f}\bar{c}_1^2 \\ F_{2c}\bar{b}_1\bar{c}_1 + F_{2e}\bar{b}_1^2 + F_{2f}\bar{c}_1^2 \\ F_{3c}\bar{b}_1\bar{c}_1 + F_{3e}\bar{b}_1^2 + F_{3f}\bar{c}_1^2 \end{pmatrix} =$$

$$= \begin{pmatrix} \frac{F_{1c}\bar{b}_1\bar{c}_1 + F_{1e}\bar{b}_1^2 + F_{1f}\bar{c}_1^2}{2(\tau+\omega i)+\eta} \\ \frac{(2(\tau+\omega i)-\tau)(F_{2c}\bar{b}_1\bar{c}_1 + F_{2e}b_1^2 + F_{2f}\ \bar{c}_1^2) + (F_{3c}\bar{b}_1\bar{c}_1 + F_{3e}\bar{b}_1^2 + F_{3f}\bar{c}_1^2)\omega}{[(2(\tau+\omega i)-\tau)^2+\omega^2]} \\ -\frac{\omega(F_{3c}\bar{b}_1\bar{c}_1 + F_{3e}\bar{b}_1^2 + F_{3f}\ c_1^2) + (2(\tau+\omega i)-\tau)(F_{2c}\bar{b}_1\bar{c}_1 + F_{2e}\bar{b}_1^2 + F_{2f}\bar{c}_1^2)}{[(2(\tau+\omega i)-\tau)^2+\omega^2]} \end{pmatrix}$$

where $\bar{b}_1$ and $\bar{c}_1$ are as above.

As previously explained, the procedure can be iterated for higher values of s. However, for the purposes of this paper, we can stop the computation at $s = 3$.

Therefore, for $t < 0$, coordinates of the variables (not far away from the steady state) can be approximated as follows

$$
\begin{aligned}
w_1 &= (\zeta - \psi i)\, e^{(\tau+\omega i)t} + (\bar{a}_2 + \bar{a}_2 i)\, e^{(\tau+\omega i)t} \\
w_2 &= (\zeta + \psi i)\, e^{(\tau+\omega i)t} + \left(\bar{b}_2 + \bar{b}_2 i\right) e^{(\tau+\omega i)t} \\
w_3 &= (\bar{c}_2 + \bar{c}_2 i)\, e^{(\tau+\omega i)t}
\end{aligned}
$$

which by Euler formulae become

$$
\begin{aligned}
w_1 &= e^{\tau t}\left[\zeta \cos(\omega t) + \psi \sin(\omega t) + (\zeta \sin(\omega t) - \psi \cos(\omega t))\, i\right] + \\
&\quad + e^{2\omega t}\left\{\left[\bar{a}_2^{(1)} \cos(2\omega t) - \bar{a}_2^{(2)} \sin(2\omega t)\right] + i\left[\bar{a}_2^{(1)} \sin(2\omega t) + \bar{a}_2^{(2)} \cos(2\omega t)\right]\right\} \\
w_2 &= e^{\tau t}\left[\zeta \cos(\omega t) - \psi \sin(\omega t) + (\zeta \sin(\omega t) + \psi \cos(\omega t))\, i\right] + \\
&\quad + e^{2\omega t}\left\{\left[\bar{b}_2^{(1)} \cos(2\omega t) - \bar{b}_2^{(2)} \sin(2\omega t)\right] + i\left[\bar{b}_2^{(1)} \sin(2\omega t) + \bar{b}_2^{(2)} \cos(2\omega t)\right]\right\} \\
w_3 &= e^{2\omega t}\left\{\left[\bar{c}_2^{(1)} \cos(2\omega t) - \bar{c}_2^{(2)} \sin(2\omega t)\right] + i\left[\bar{c}_2^{(1)} \sin(2\omega t) + \bar{c}_2^{(2)} \cos(2\omega t)\right]\right\}
\end{aligned}
$$

provided that $\bar{a}_2 = \bar{a}_2^{(1)} + \bar{a}_2^{(2)} i$, $\bar{b}_2 = \bar{b}_2^{(1)} + \bar{b}_2^{(2)} i$, and $\bar{c}_2 = \bar{c}_2^{(1)} + \bar{c}_2^{(2)} i$.

Now, let us rely on the principle of superposition, implying that, for a generic autonomous system $\dot{W} = g(W)$, if $W_1 + W_2 i$ is a complex solution, then W_1 and W_2 are real solutions of the system. In our case, we have

$$
\begin{aligned}
w_{11} &= e^{\tau t}\left[\zeta \cos(\omega t) + \psi \sin(\omega t)\right] + e^{2\omega t}\left[\bar{a}_2^{(1)} \cos(2\omega t) - \bar{a}_2^{(2)} \sin(2\omega t)\right] \\
w_{21} &= e^{\tau t}\left[\zeta \cos(\omega t) - \psi \sin(\omega t)\right] + e^{2\omega t}\left[\bar{b}_2^{(1)} \cos(2\omega t) - \bar{b}_2^{(2)} \sin(2\omega t)\right] \\
w_{31} &= e^{2\omega t}\left[\bar{c}_2^{(1)} \cos(2\omega t) - \bar{c}_2^{(2)} \sin(2\omega t)\right]
\end{aligned}
$$

and

$$
\begin{aligned}
w_{12} &= e^{\tau t}\left[(\zeta \sin(\omega t) - \psi \cos(\omega t))\right] + e^{2\omega t}\left[\bar{a}_2^{(1)} \sin(2\omega t) + \bar{a}_2^{(2)} \cos(2\omega t)\right] \\
w_{22} &= e^{\tau t}\left[(\zeta \sin(\omega t) + \psi \cos(\omega t))\right] + e^{2\omega t}\left[\bar{b}_2^{(1)} \sin(2\omega t) + \bar{b}_2^{(2)} \cos(2\omega t)\right] \\
w_{32} &= e^{2\omega t}\left[\bar{c}_2^{(1)} \sin(2\omega t) + \bar{c}_2^{(2)} \cos(2\omega t)\right]
\end{aligned}
$$

Therefore, near the unstable manifold, the solution of the generic system $\dot{W} = g(W)$ can be characterized as follows

$$
\begin{pmatrix} w_1 \\ w_2 \\ w_3 \end{pmatrix} = d_1 \begin{pmatrix} w_{11} \\ w_{21} \\ w_{31} \end{pmatrix} + d_2 \begin{pmatrix} w_{12} \\ w_{22} \\ w_{32} \end{pmatrix}
$$

where $(d_1, d_2) = (0, 1)$ or $(1, 0)$.

Therefore, going back to the solutions of our system of differential equations along the unstable and stable manifolds, we can write

$$
w_1 = \left\{
\begin{array}{lr}
\xi e^{-\eta t} + a_2 e^{-2\eta t} & t \geq 0 \\
d_1\left\{e^{\tau t}\left[\zeta \cos(\omega t) + \psi \sin(\omega t)\right] + e^{2\omega t}\left[\bar{a}_2^{(1)} \cos(2\omega t) - \bar{a}_2^{(2)} \sin(2\omega t)\right]\right\} + & t \leq 0 \\
d_2\left\{e^{\tau t}\left[(\zeta \sin(\omega t) - \psi \cos(\omega t))\right] + e^{2\omega t}\left[\bar{a}_2^{(1)} \sin(2\omega t) + \bar{a}_2^{(2)} \cos(2\omega t)\right]\right\} &
\end{array}
\right\}
$$

$$w_2 = \begin{cases} b_2 e^{-2\eta t} & t \geq 0 \\ d_1 \left\{ e^{\tau t} \left[\zeta \cos(\omega t) - \psi \sin(\omega t) \right] + e^{2\omega t} \left[\bar{b}_2^{(1)} \cos(2\omega t) - \bar{b}_2^{(2)} \sin(2\omega t) \right] \right\} + & t \leq 0 \\ d_2 \left\{ e^{\tau t} \left[(\zeta \sin(\omega t) + \psi \cos(\omega t)) \right] + e^{2\omega t} \left[\bar{b}_2^{(1)} \sin(2\omega t) + \bar{b}_2^{(2)} \cos(2\omega t) \right] \right\} & \end{cases}$$

$$w_2 = \begin{cases} c_2 e^{-2\eta t} & t \geq 0 \\ d_1 \left\{ e^{2\omega t} \left[\bar{c}_2^{(1)} \cos(2\omega t) - \bar{c}_2^{(2)} \sin(2\omega t) \right] \right\} + & t \leq 0 \\ d_2 \left\{ e^{2\omega t} \left[\bar{c}_2^{(1)} \cos(2\omega t) - \bar{c}_2^{(2)} \sin(2\omega t) \right] + \left[\bar{c}_2^{(1)} \sin(2\omega t) + \bar{c}_2^{(2)} \cos(2\omega t) \right] \right\} & \end{cases}$$

At $t = 0$, $w_1 = w_2 = w_3 = 0$. Thus, simplifying and solving, we obtain the following three dimensional system in the unknowns (ξ, ψ, ζ)

$$\begin{aligned} \xi + a_2 &= d_1 \left(\zeta + \bar{a}_2^{(1)} \right) \bar{a}_2^{(1)} + d_2 \\ b_2 &= d_1 \left[\psi + \bar{b}_2^{(1)} \right] + d_2 \left[\zeta + \bar{b}_2^{(1)} \right] \\ c_2 &= d_1 \left[\zeta + \bar{c}_2^{(1)} \right] + d_2 \left[-\psi + \bar{c}_2^{(1)} \right] \end{aligned}$$

Recalling the values of the various coefficients obtained above, and taking $(d_1, d_2) = (1, 0)$, we finally derive the surface

$$\xi = \frac{F_{1c}\psi\zeta + F_{1e}\psi^2 + F_{1f}\zeta^2}{(4\tau - \eta)^2 + \omega^2}(2\tau - \eta) - \frac{F_{1d}}{\eta} \frac{(4\eta^2 + 4\eta\tau + \tau^2 + \omega^2)}{(F_{2d} + F_{3d})(\tau - \omega + 2\eta)}(\psi + \zeta) \quad \text{(A.24)}$$

which represents combinations of the (ξ, ψ, ζ) parameters corresponding to a family of homoclinic orbits.

Proposition 3 can now be clarified. It implies that, given the structural parameters of the model (belonging to the non-empty subset satisfying the requirement H.1 of the Shilnikov theorem), and given the constants φ_1, φ_2 and φ_3 in the choice of the eigenvectors, then we can select the value of the externality factor $\gamma = \gamma_h$ such that (A.24) is satisfied and one homoclinic orbit emerges. By topological equivalence, the results also apply to system $\mathcal{S}$.

To complete the information, the explicit expressions of the F_{ij} coefficients necessary for the computation of (A.24) are the following

$$\begin{aligned} F_{1c} &= V^* z_1 + [V^* \tfrac{u^*}{x^*} + \tfrac{\delta(1-\beta+\gamma)}{1-\beta}] z_2 - z_3 - v_3 z_1) \\ F_{1d} &= \tfrac{1}{2} V^* u_1^2 + [V^* \tfrac{u^*}{x^*} + \tfrac{\delta(1-\beta+\gamma)}{1-\beta}] u_1 u_2 - u_1 u_3 \\ F_{1e} &= \tfrac{1}{2} V^* - v_3 \\ F_{1f} &= \tfrac{1}{2} V^* z_1^2 + [V^* \tfrac{x^*}{u^*} + \tfrac{\delta(1-\beta+\gamma)}{1-\beta}] z_1 z_2 - z_1 z_3 \\ F_{2d} &= \eta u_2^2 - u_1 u_3 \\ F_{3d} &= \tfrac{\beta-\sigma}{\sigma} V^* q^* \left[\tfrac{1}{2} \tfrac{(\beta-1)(\beta-2)}{\beta x^*} + \tfrac{1}{2x^* u^{*-1+\beta}} + \tfrac{1-\beta}{\beta x^* u^*} \right] u_1^2 + u_3^2 + \tfrac{\beta-\sigma}{\beta\sigma} V^* \left[-\tfrac{1}{x^* u^*} + 1 \right] u_1 u_3 \end{aligned}$$

where $V^* = \beta(\beta - 1) x^{*\beta-2} u^{*1-\beta}$.

A.4. TVC and chaotic paths

The TVC requires the present value of the state variables to converge to zero as the planning horizon proceeds towards infinity. Benhabib and Perli (1994) show that, at the steady state

$P^* \equiv (x^*, u^*, q^*)$ the TVC holds provided that $\theta \in \Theta_1 \cup \Theta_2$. Moreover, Mattana and Venturi (1999) and Nishimura and Shigoka (2006) show that the TVC is also satisfied in case the economy converges to a Hopf cycle, well located in the $\mathbb{R}^3$ ambient space, provided that the solution trajectories are in a convenient small neighborhood of the steady state. For the case of solution trajectories resulting in Shilnikov chaos, we proceed as follows. First, we observe that an extension in $\mathbb{R}^3$ of the argument in Mattana and Venturi (1999) and Nishimura and Shigoka (2006) can be used to assure that (A.24) is always satisfied along the homoclinic orbit. More formally, assume we can appropriately choose the scaling factors φ_i $i = 1, 2, 3$ so that the homoclinic orbit is contained in an open sphere with radius r around the steady state $P^* \equiv (x^*, u^*, q^*)$ such that $0 < u_{|r} < 1$. Then along every homoclinic orbit contained in the sphere, the present value of the state variables will always tend to zero as the planning horizon proceeds towards infinity. Secondly, we need to show that $0 < u_t < 1$ along a specific chaotic paths emerging after the rupture of the homoclinic orbit. In this regard, it is sufficient to recall from Theorem 1, that the chaotic trajectory is confined to exist in a small neighborhood of the homoclinic orbit.

References

Acemoglu, D., Jackson, M.O., 2015. History, expectations, and leadership in the evolution of social norms. Rev. Econ. Stud. 82, 423–456.

Antoci, A., Galeotti, M., Russu, P., 2014. Global analysis and indeterminacy in a two-sector growth model with human capital. Int. J. Econ. Theory 10, 313–338.

Barnett, W.A., Ghosh, T., 2014. Stability analysis of Uzawa–Lucas endogenous growth model. Econ. Theory Bull. 2, 33–44.

Bella, G., Mattana, P., 2014. Global indeterminacy of the equilibrium in the Chamley model of endogenous growth in the vicinity of a Bogdanov–Takens bifurcation. Math. Soc. Sci. 71, 69–79.

Benhabib, J., Eusepi, S., 2005. The design of monetary and fiscal policy: a global perspective. J. Econ. Theory 123, 40–73.

Benhabib, J., Farmer, R., 1996. Indeterminacy and sector-specific externalities. J. Monet. Econ. 17, 421–443.

Benhabib, J., Farmer, R., 1999. Indeterminacy and sunspots in macroeconomics. In: Taylor, J.B., Woodford, M. (Eds.), Handbook of Macroeconomics, pp. 387–448. Amsterdam.

Benhabib, J., Perli, R., 1994. Uniqueness and indeterminacy: on the dynamics of endogenous growth. J. Econ. Theory 63, 113–142.

Benhabib, J., Perli, R., Xie, D., 1994. Monopolistic competition, indeterminacy and growth. Res. Econ. 48, 279–298.

Benhabib, J., Meng, Q., Nishimura, K., 2000. Indeterminacy under constant returns to scale in multisector economies. Econometrica 68, 1541–1548.

Benhabib, J., Schmitt-Grohé, S., Uribe, M., 2001. The perils of Taylor rules. J. Econ. Theory 96, 40–69.

Benhabib, J., Nishimura, K., Shigoka, T., 2008. Bifurcation and sunspots in the continuous time equilibrium model with capacity utilization. Int. J. Econ. Theory 4, 337–355.

Bethmann, D., Reiß, M., 2012. Simplifying numerical analyses of Hamilton–Jacobi–Bellman equations. J. Econ. 107, 101–128.

Boldrin, M., Nishimura, K., Shigoka, T., Yano, M., 2001. Chaotic equilibrium dynamics in endogenous growth models. J. Econ. Theory 96, 97–132.

Boucekkine, R., Ruiz-Tamarit, R., 2008. Special functions for the study of economic dynamics: the case of the Lucas–Uzawa model. J. Math. Econ. 44, 33–54.

Boucekkine, R., Martinez, B., Ruiz-Tamarit, R., 2008. A note on global dynamics and imbalance effects in the Lucas–Uzawa model. Int. J. Econ. Theory 4, 503–518.

Brito, P., Venditti, A., 2010. Local and global indeterminacy in two-sector models of endogenous growth. J. Math. Econ. 46, 893–911.

Caballé, J., Santos, M.S., 1993. On endogenous growth with physical and human capital. J. Polit. Econ. 101, 1042–1067.

Chamley, C., 1993. Externalities and dynamics in models of learning or doing. Int. Econ. Rev. 34, 583–609.

Chen, B., Zhou, T., 2011. Shilnikov homoclinic orbits in two classes of 3D autonomous nonlinear systems. Int. J. Mod. Phys. B 25, 2697–2712.

Chilarescu, C., Viasu, I., 2016. A closed-form solution of a two-sector endogenous growth model with habit formation. Aust. Econ. Pap. 55, 112–127.
Coury, T., Wen, T., 2009. Global indeterminacy in locally determinate real business cycle models. Int. J. Econ. Theory 5, 49–60.
Faig, M., 1995. A simple economy with human capital: transitional dynamics, technology shocks, and fiscal policies. J. Macroecon. 17, 421–446.
Farmer, R., 2016. The evolution of endogenous business cycles. Macroecon. Dyn. 20, 544–557.
Garcia-Castrillo, P., Sanso, M., 2000. Human capital and optimal policy in a Lucas-type model. Rev. Econ. Dyn. 3, 757–770.
Gardini, L., Sushko, I., Naimzada, A., 2008. Growing through chaotic intervals. J. Econ. Theory 143, 541–557.
Khan, M.A., Mitra, T., 2005. On topological chaos in the Robinson–Solow–Srinivasan model. Econ. Lett. 88, 127–133.
Kopell, N., Howard, L.N., 1975. Bifurcations and trajectories joining critical points. Adv. Appl. Math. 18, 306–358.
Krugman, P., 1991. Increasing returns and economic geography. J. Polit. Econ. 99, 483–499.
Kuznetsov, Y.A., 2004. Elements of Applied Bifurcation Theory. Springer-Verlag, New York.
Lucas, R., 1988. On the mechanics of economic development. J. Monet. Econ. 22, 3–42.
Lucas, R., Moll, B., 2014. Knowledge growth and the allocation of time. J. Polit. Econ. 122, 1–51.
Manuelli, R., Seshadri, A., 2014. Human capital and the wealth of nations. Am. Econ. Rev. 104, 2736–2762.
Matsuyama, K., 1991. Increasing returns, industrialization, and indeterminacy of equilibrium. Q. J. Econ. 106, 617–650.
Matsuyama, K., 1999. Growing through cycles. Econometrica 67, 335–347.
Matsuyama, K., 2001. Growing through cycles in an infinitely lived agent economy. J. Econ. Theory 100, 220–234.
Mattana, P., Nishimura, K., Shigoka, T., 2009. Homoclinic bifurcation and global indeterminacy of equilibrium in a two-sector endogenous growth model. Int. J. Econ. Theory 5, 1–23.
Mattana, P., Venturi, B., 1999. Existence and stability of periodic solutions in the dynamics of endogenous growth. Int. Rev. Econ. Bus. 46, 259–284.
Mino, K., 2004. Human capital formation and patterns of growth with multiple equilibria. In: Boldrin, M., Chen, B., Wang, P. (Eds.), Human Capital, Trade, and Public Policy in Rapidly Growing Economies: From Theory to Empirics. In: Academia Studies in Asian Economies. Edward Elgar, Cheltenham, UK, pp. 42–64.
Mitra, T., 2001. A sufficient condition for topological chaos with an application to a model of endogenous growth. J. Econ. Theory 96, 133–152.
Mitra, T., Nishimura, K., 2001a. Introduction to intertemporal equilibrium theory: indeterminacy, bifurcations, and stability. J. Econ. Theory 96, 1–12.
Mitra, T., Nishimura, K., 2001b. Discounting and long-run behavior: global bifurcation analysis of a family of dynamical systems. J. Econ. Theory 96, 256–293.
Mortensen, D.T., 1999. Equilibrium unemployment dynamics. Int. Econ. Rev. 40, 889–914.
Mulligan, C.B., Sala-i-Martin, X., 1993. Transitional dynamics in two-sector models of endogenous growth. Q. J. Econ. 103, 739–773.
Naz, R., Chaudhry, A., Mahomed, F.M., 2016. Closed-form solutions for the Lucas–Uzawa model of economic growth via the partial Hamiltonian approach. Commun. Nonlinear Sci. Numer. Simul. 30, 299–306.
Nishimura, K., Sorger, G., Yano, M., 1994. Ergodic chaos in optimal growth models with low discount rates. Econ. Theory 4, 705–717.
Nishimura, K., Shigoka, T., 2006. Sunspots and Hopf bifurcations in continuous time endogenous growth models. Int. J. Econ. Theory 2, 199–216.
Nishimura, K., Yano, M., 1995. Nonlinear dynamics and chaos in optimal growth: an example. Econometrica 63, 981–1001.
Shang, D., Han, M., 2005. The existence of homoclinic orbits to saddle-focus. Appl. Math. Comput. 163, 621–631.
Shilnikov, L.P., 1965. A case of the existence of a denumerate set of periodic motions. Sov. Math. Dokl. 6, 163–166.
Sniekers, F., 2016. Persistence and volatility of Beveridge cycles. Int. Econ. Rev. forthcoming.
Wälde, K., 2005. Endogenous growth cycles. Int. Econ. Rev. 46, 867–894.
Xie, D., 1994. Divergence in economic performance: transitional dynamics with multiple equilibria. J. Econ. Theory 63, 97–112.